UNIVERSIDADE FEDERAL DO CEARÁ

CENTRO DE TECHNOLOGIA

DEPARTAMENTO DE ENGENHARIA ELÉTRICA

PROGRAMA DE PÓS-GRADUAÇÃO EM ENGENHARIA ELÉTRICA

THIAGO ALVES LIMA

CONTRIBUTIONS ON THE STABILITY ANALYSIS OF THE SIMPLIFIED DEAD-TIME COMPENSATOR WITH SATURATING ACTUATORS

FORTALEZA

2018

THIAGO ALVES LIMA

CONTRIBUTIONS ON THE STABILITY ANALYSIS OF THE SIMPLIFIED DEAD-TIME COMPENSATOR WITH SATURATING ACTUATORS

Dissertação apresentada ao Curso de Engenharia Elétrica do Programa de Pós-graduação em Engenharia Elétrica do Centro de Technologia da Universidade Federal do Ceará, como requisito parcial à obtenção do título de mestre em Engenharia Elétrica. Área de Concentração: Sistemas de Energia Elétrica

Orientador: Prof. Dr. Fabrício Gonzalez Nogueira

Coorientador: Prof. Dr. Bismark Claure Torrico

FORTALEZA

2018

Dados Internacionais de Catalogação na Publicação
Universidade Federal do Ceará
Biblioteca Universitária
Gerada automaticamente pelo módulo Catalog, mediante os dados fornecidos pelo(a) autor(a)

A482c Alves Lima, Thiago.
Contributions on the stability analysis of the simplified dead-time compensator with saturating actuators / Thiago Alves Lima. – 2018.
89 f. : il. color.

Dissertação (mestrado) – Universidade Federal do Ceará, Centro de Tecnologia, Programa de Pós-Graduação em Engenharia de Transportes, Fortaleza, 2018.
Orientação: Prof. Dr. Fabrício Gonzalez Nogueira.
Coorientação: Prof. Dr. Bismark Claure Torrico.

1. Compensador de Tempo Morto Simplificado. 2. Preditor de Smith Filtrado. 3. Saturação do Atuador. 4. Estabilidade. I. Título.

CDD 388

THIAGO ALVES LIMA

CONTRIBUTIONS ON THE STABILITY ANALYSIS OF THE SIMPLIFIED DEAD-TIME COMPENSATOR WITH SATURATING ACTUATORS

Dissertação apresentada ao Curso de Engenharia Elétrica do Programa de Pós-graduação em Engenharia Elétrica do Centro de Technologia da Universidade Federal do Ceará, como requisito parcial à obtenção do título de mestre em Engenharia Elétrica. Área de Concentração: Sistemas de Energia Elétrica

Aprovada em 31 de Janeiro de 2018.

EXAMINATION BOARD

Prof. Dr. Fabrício Gonzalez Nogueira (Orientador)
Universidade Federal do Ceará (UFC)

Prof. Dr. Bismark Claure Torrico (Coorientador)
Universidade Federal do Ceará (UFC)

Prof. Dr. Wilkley Bezerra Correia
Universidade Federal do Ceará (UFC)

Prof. Dr. Guilherme de Alencar Barreto
Universidade Federal do Ceará (UFC)

To my mom, Antonia, for being the greatest supporter of my academic life and to my family for being my safe harbor.

ACKNOWLEDGEMENTS

I would first like to thank God for blessing me with great opportunities and knowledge.

Second, a special thanks to my mom, Antonia, for her continuous support and for teaching me to never give up on my goals.

Thanks to my family and friends who helped me to go through the hard moments during the development of this thesis.

Thank you to Dr. Fabrício Nogueira and Dr. Bismark Torrico, who patiently taught me the subjects on control systems.

Thank you to my colleague and friend Magno, who greatly helped me in the development of this research.

Lastly, thanks to FUNCAP for providing financial support.

"Never forget what you are, for surely the world will not. Make it your strength. Then it can never be your weakness. Armour yourself in it, and it will never be used to hurt you."

(Tyrion Lannister in *A Song of Ice and Fire* by George R.R. Martin)

RESUMO

Essa dissertação apresenta análise de estabilidade robusta e nominal do *Simplified Dead-time Compensator* (SDTC) na presença de saturação do atuador para processos estáveis e integradores com atraso de transporte. Tal análise é concebida por meio de LMIs obtidas da condição de estabilidade de Lyapunov e da condição do setor, com análise de desempenho baseada no ganho $\mathscr{L}_2$. A principal vantagem do SDTC é que uma estratégia *anti-windup* pode ser implementada apenas pela adição do modelo da saturação do atuador à estrutura de controle. O procedimento de ajuste juntamente com comparações entre a estratégia proposta e outros controladores de tempo-morto *anti-windup*, incluindo um MPC com restrições, são apresentados nos exemplos de simulação. Em adição, resultados experimentais numa unidade de tratamento intensivo neonatal são apresentados para validar a utilidade do SDTC.

Palavras-chave: Compensador de Tempo Morto Simplificado. Preditor de *Smith* Filtrado. Saturação do Atuador. Estabilidade.

ABSTRACT

This thesis presents nominal and robust stability analysis of the simplified dead-time compensator (SDTC) with actuator saturation for stable and integrative dead-time processes. Such analysis is carried out under LMI framework obtained from the Lyapunov stability and the sector boundedness conditions with performance analysis based on $\mathscr{L}_2$ gain. The main advantage of the SDTC is that an anti-windup strategy can be implemented just by addition of the actuator saturation model to the control structure. Tuning procedure along with comparison between the proposed strategy and other anti-windup DTC controllers, including constrained MPC, are discussed with simulation examples. In addition, experimental results on a neonatal intensive care unit are presented in order to validate the usefulness of the SDTC.

Keywords: Simplified Dead-time Compensator. Filtered Smith Predictor. Actuator Saturation. Stability

LIST OF FIGURES

LIST OF TABLES

LIST OF ABBREVIATIONS AND ACRONYMS

AWSDTC	Anti-windup Simplified Dead-time Compensator
DTCs	Dead-time Compensators
FOPDT	First Order Plus Dead-time
FSP	Filtered Smith Predictor
LMI	Linear Matrix Inequality
MIMO	Multiple-input Multiple-output
MPCs	Model-based Predictive Controllers
NCSs	Networked Control Systems
NICU	Neonatal Intensive Care Unit
PI	Proportional Integral
PID	Proportional Integral Derivative
SDTC	Simplified Dead-time Compensator
SISO	Single-input Single-output
SOPDT	Second Order Plus Dead-time
SP	Smith Predictor
TCP	Transmission Control Protocol

LIST OF SYMBOLS

$\star$	Symmetric blocks in the expression of a matrix.
$\mathbb{Z}$	The set of integer numbers.
$\mathbb{Z}^+$	The set of nonnegative integer numbers.
$\mathbb{N}$	The set of natural numbers.
$\mathbb{R}$	The set of real numbers.
$\mathbb{N}$	The set of natural numbers.
k	Discrete-time sample.
t	Continuous time.
u	Input of a system.
y	Output of a system.
γ	$\mathscr{L}_2$ gain.
A^T	The transpose of matrix A.
A^{-1}	The inverse of matrix A.
$A > 0$	Means that matrix A is positive definite.
$A \geq 0$	Means that matrix A is positive semidefinite.
$A < 0$	Means that matrix A is negative definite.
$A \leq 0$	Means that matrix A is negative semidefinite.
$diag(A_1, A_2, ..., A_m)$	Denotes the block-diagonal matrix formed with matrices $A_i, i = 1, ..., m$.
$col\{x_1, x_2\}$	Denotes the column vector $\begin{bmatrix} x_1^\mathsf{T} & x_1^\mathsf{T} \end{bmatrix}^\mathsf{T}$.

CONTENTS

1 INTRODUCTION

1.1 Time-delay systems

Time-delay appears in a wide variety of real-word processes from biology to economics and communication systems. The source of delay can be related to many causes such as mass or energy transportation in the process. For instance, in the case of economics, time-delay looks quite natural since there exists time intervals between information acquisition, decision making and their effects in the market.

Time-delay can appear either in the state, control input or in the measured plant output, and is usually associated to a source of instability in the closed-loop. Therefore, stability analysis of control structures for such systems is of theoretical importance. Systems with constant delay have received most of the attention in the last decade, whereas the problem of time-varying delay started to gain more importance in recent years due to the rise of Networked Control Systems (NCSs).

Networked control systems are distributed systems in which data is transmitted between actuators, sensors and controllers through communication networks, often relying on protocols such as Transmission Control Protocol (TCP). This research area is identified as a key for the future of control systems (LAMNABHI-LAGARRIGUE *et al.*, 2017; HESPANHA *et al.*, 2007) due to its diverse application; networks of mobile vehicles, smart grids and the healthcare industry are a few examples. A general structure of a networked output-feedback control system is depicted in Figure 1, where $y(t)$ is the process measured output, $u(t)$ is the plant input and τ is a time-varying delay due to the communication network.

1.2 Actuator Saturation

Besides time-delay, another major topic in control systems is actuator saturation. Although most control systems projects do not consider boundaries in the amplitude or rate of the process control input, all real-life actuators present such limitations. For instance, electrical actuators have voltage limits, whereas there exist limitations on both volume and rate of flow in hydraulic actuators. This can also be a cause of instability in the closed-loop system, due to a phenomenon known as windup. Instability is, however, only one of the possible consequences of this condition. Therefore, it is necessary to include strategies which avoid windup and its

Figure 1 – General networked output-feedback control system.

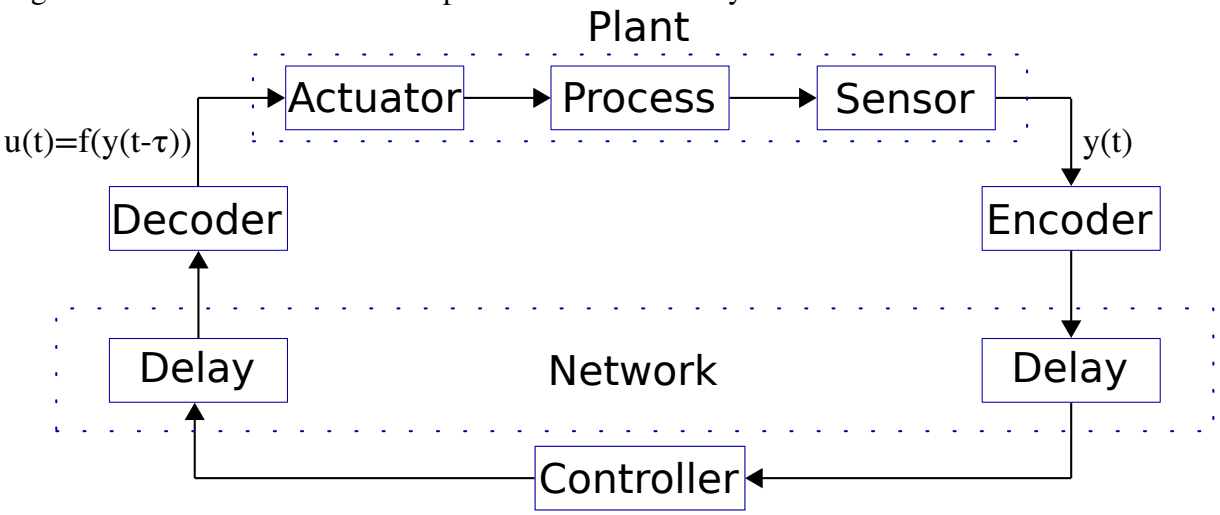

Source: The author.

undesirable consequences in the control loop, as contextualized as follows.

Windup occurs when the model of the saturation to the plant input is unknown, thus leading the states of the controller to be wrongly updated (KOTHARE *et al.*, 1994) and causing major problems to the control system. Especially, this can make the output of the plant oscillatory or unstable. In other cases, the set-point tracking response can become painfully slow. The origin of the term windup comes from the cases of Proportional Integral (PI) and Proportional Integral Derivative (PID) controllers, in which the integral state "winds up" to large values during saturation events; the associated energy is later dissipated, causing the problems described above. It is import to note that although early practice control engineers associated this phenomenon to integral action, it was latter discovered that slow or unstable modes in the control system can also cause windup problems.

In addition to avoiding windup consequences, research effort on saturated systems is of interest because considering limitations on the control signal can lead to the synthesis of more economic control laws. Moreover, in the historical perspective, saturated actuators have had implications in many tragedies such as aircraft crashes and the Chernobyl nuclear power station disaster (TARBOURIECH; TURNER, 2009). Thus, it is mandatory to guarantee stability of control structures operating at such conditions. However, this is not an easy task and the necessary mathematical rigor to make such guarantees was mainly developed in the 1990's with the development of the Linear Matrix Inequality (LMI) theory, which is going to be heavily employed in this work.

1.3 Related Work

Dead-time Compensators (DTCs) have been widely studied for about the past 25 years mainly due to their ability to improve the performance of classical PI and/or PID controllers when the process presents time-delay between the input and output. The first DTC was proposed in Smith (1957), also known in literature as the Smith Predictor (SP). The proposal presented limitations, since its application is restricted to open-loop stable plants, while the disturbance rejection response is dominated by the slow poles of the plant (NORMEY-RICO; CAMACHO, 2007). Since then several extensions have been proposed to improve robustness, disturbance rejection, and measurement noise attenuation. Some works intended to improve the SP robustness and disturbance rejection of stable and/or integrative dead time processes can be found in Astrom *et al.* (1994), Mataušek and Micić" (1996), Mataušek and Micić (1999), Rao *et al.* (2007), Kaya (2003), Rao and Chidambaram (2008), Normey-Rico and Camacho (2008), Kirtania and Choudhury (2012). Nevertheless, the study of the effect of the measurement noise is less common. In García *et al.* (2006), Albertos and García (2009), García and Albertos (2008) the noise effect in DTC structures is shown using simulations. In Santos *et al.* (2010), an analysis for stable, integrative and unstable dead-time processes using the Filtered Smith Predictor (FSP) with improved noise attenuation was presented. However, the aforementioned works are not concerned with actuator saturation, which is common in practical applications and can cause windup problems due to differences between the controller output and the actual plant input. An applicable solution of the modified Smith predictor (MATAUŠEK; MICIĆ", 1996; MATAUŠEK; MICIĆ, 1999), with anti-windup was proposed in Mataušek and Ribić (2012), although an optimization procedure is necessary to define some desired robustness and noise sensitivity constraints.

In Zhang and Jiang (2008) and Flesch *et al.* (2017) anti-windup structures for the FSP were proposed. In Huba (2013) a predictive disturbance observer based filtered PI control for First Order Plus Dead-time (FOPDT) processes is presented and in Huba (2015) the tuning for integrative plants with dead time based on robustness and performance criteria is analysed. Another alternative to deal with constraints lies in the use of Model-based Predictive Controllers (MPCs) (CAMACHO; BORDONS, 2004; NORMEY-RICO; CAMACHO, 2007). However, in the MPC case a constrained quadratic problem needs to be solved at each sampling time.

In Torrico *et al.* (2013), simple tuning rules were proposed for the FSP applied to the control of stable, integrative, and unstable first-order plus dead-time processes. The primary

controller is free from integral action, differently from the traditional FSP, and ensures good trade-off among disturbance rejection, robustness, and noise attenuation. The results were better than those proposed by Santos *et al.* (2010). In Huba and Tapak (2011), a control structure equivalent to that of Torrico *et al.* (2013) (with addition of anti-windup action) was presented. Nevertheless, the tuning of the proposed structure was limited for open-loop stable systems only.

In Torrico *et al.* (2016), the results obtained in Torrico *et al.* (2013) were extended to the case of multiple-delay Single-input Single-output (SISO) systems of any model order, namely Simplified Dead-time Compensator (SDTC). Despite of the good results in the presence of nonlinearity saturation, stability of the proposed scheme was not studied.

1.4 The Present Work

In this thesis the anti-windup characteristics of the SDTC are further studied, while stability and performance are analysed using LMI theory. Simulation results are used to analyse the tuning and establish a fair comparison with other anti-windup DTC presented in Zhang and Jiang (2008), Flesch *et al.* (2017) and also a constrained MPC. Furthermore, in order to test the applicability of the proposed controller, an experiment was performed to control the temperature in a Neonatal Intensive Care Unit (NICU). This work has the following specific objectives:

- To proof the nominal stability of the SDTC in the presence of actuator saturation.
- To proof robust stability of the SDTC under actuator saturation for the cases of norm-bounded and polytopic uncertainties in the process fast-model. In addition to these uncertainties, to consider the process delay to be unknown, bounded, and possibly time-varying, which can be even more harmful than constant delays.
- To use simulations to establish useful rules for the tuning of the anti-windup SDTC and demonstrate the good performance of the control structure by comparison with other anti-windup strategies.
- To use an experimental result to prove the real-life usefulness of the anti-windup SDTC.

1.5 Outline

The rest of this thesis is organized as follows.

- In Chapter 2, the mathematical preliminaries necessary to establish stability

and performance conditions in the presence of actuator saturation are presented. To comply with this goal, basic knowledge in LMIs manipulation is initially constructed. Subsequently, concepts on the Lyapunov stability of linear systems with and without delays are presented. The final Section of the Chapter is devoted to present essential concepts on the stability of systems with actuator saturation.

- Chapter 3 starts with a review of the SDTC structure. Later, its anti-windup characteristics are explained and the structure is extended to the anti-windup SDTC (AWSDTC) case by means of a simple addition to the control structure.
- Chapter 4 is a collection of nominal and robust stability results given in the form of corollaries. Thorough proof of such statements are constructed throughout the text under the LMI framework.
- Results are presented in Chapter 5, with simulation examples showing the effectiveness of the Anti-windup Simplified Dead-time Compensator (AWSDTC) structure. Experimental data for the temperature control of a neonatal incubator are discussed.
- Finally, concluding remarks are brought in the last chapter of this thesis. Contributions are summarized whereas future work is listed.

2 THEORETICAL PRELIMINARIES

In this Chapter, the preliminary knowledge necessary to proof stability of the SDTC under actuator saturation is constructed. Initially, the main properties in LMIs manipulation are presented in Section 2.1. In order to access stability, the Lyapunov stability of linear systems and the sector boundness condition for the stability of systems with actuator saturation are presented in Sections 2.2 and 2.3, respectively. Section 2.3 also presents the definition of the $\mathscr{L}_2$ gain, which is used as a performance indicator of the anti-windup strategy.

2.1 Linear Matrix Inequalities

A wide variety of control problems can be described in the format of LMIs. These are matrix inequalities which have an affine relationship with a set of matrix variables. While most of the earlier works on Lyapunov stability were formulated using algebraic Riccati equations, the use of LMIs became popular in the 1990's due to the development of efficient interior point method algorithms. LMIs soon became a powerful tool in robust control synthesis in the presence of structured uncertainties (CHILALI; GAHINET, 1996), and later in the presence of actuator saturation (WESTON; POSTLETHWAITE, 2000). There exist many packages which provide solutions to LMIs by using convex optimization, such as the Yalmip toolbox (LOFBERG, 2004).

The main attractions for the use of LMI are listed as (SKOGESTAD; POSTLETHWAITE, 2005)

- LMIs can be used to solve problems which involve several matrix variables.
- Their manipulation is flexible, thus a wide variety of problems can be posed as LMIs in a very straightforward way.
- Restrictions that cause traditional formulations to either fail or struggle to find a solution can often be removed by using LMIs. Furthermore, LMIs can aid their extension to more general scenarios.
- Many control problems can be united into a single LMI.

2.1.1 Fundamentals of LMIs

After explaining the fundamental reasons for using LMIs, the following text explains their concepts.

Definition 2.1.1 *A linear matrix inequality (LMI) is described by the following expression (BOYD et al., 1994)*

$$F(x) \triangleq F_0 + \sum_{i=1}^{m} x_i F_i > 0. \tag{2.1}$$

Where

- $F_i = F_i^{\mathsf{T}} \in \mathbb{R}^{nxn}$ *are real given symmetric matrices.*
- $x = [x_i, ..., x_m] \in \mathbb{R}^m$ *is the decision variable.*
- *The inequality* > 0 *denotes that* $F(x)$ *is positive definite, i.e. all eigenvalues are positive. Thus,* $u^{\mathsf{T}} F(x)u > 0$ *for all* $u \in \mathbb{R}^n, u \neq 0$*. Non-strict LMIs are defined by using the symbol* ≥ 0*.*

The LMI problem in Equation (2.1) is to find x such that $F(x)$ holds. This is a convex constraint on x, i.e., the set $\{x|F(x) > 0\}$ is convex. Multiple LMIs $F_1(x) > 0, F_2(x) > 0, ..., F_m(x) > 0$, can be expressed as a single LMI of the form:

$$F(x) = \begin{bmatrix} F_1(x) & \cdots & 0 \\ \vdots & \ddots & \vdots \\ 0 & \cdots & F_m(x) \end{bmatrix} > 0, \tag{2.2}$$

which is also a convex set, as illustrated in Figure 2.

Figure 2 – Convex set of LMIs.

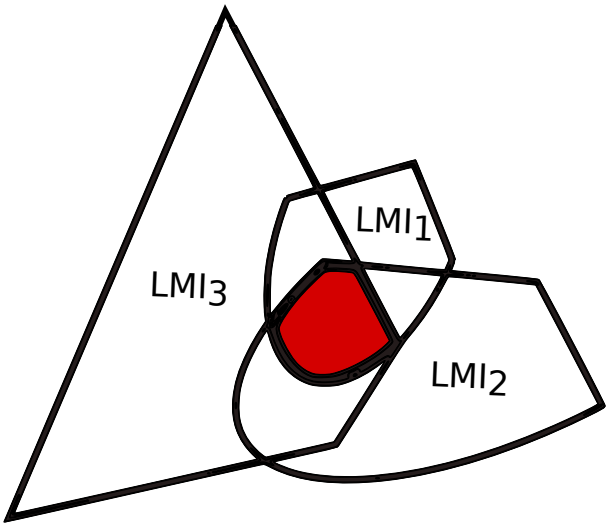

Source: The author.

Convex optimization solution may be arranged in two main problems to be solved under the LMI framework. The first one is called a feasibility problem and consists of either

finding any x_{feas} such that $F(x_{feas}) > 0$ holds or determining that the problem is infeasible. The second is called an optimization problem (also called eigenvalue problem). This consists of minimizing (or maximizing) some convex cost function of the unknown variable x subject to LMI constraints as

$$\min \Gamma(x) \text{ such that } F(x) > 0. \tag{2.3}$$

Important tricks used in the manipulation of LMIs (useful for the stability proofs provided in this work) are explained in the rest of this section.

2.1.1.1 Congruence Transformation

Consider a real positive definite matrix $P \in \mathbb{R}^{nxn}$. It is known that pre- and postmultiplication of P by a full rank matrix $W \in \mathbb{R}^{nxn}$, and its transpose, does not affect the definitess of P. Then, the following Equation illustrates the process of congruence transformation

$$WPW^{\intercal} > 0. \tag{2.4}$$

This trick is often used along with change of variables to eliminate nonlinearities in matrix inequalities, as illustrated in Example 1.

2.1.1.2 Change of Variables

Consider the Example 1 to explain the tricks of change of variable and also congruence transformation.

Example 1 *Consider the problem of finding a state-feedback matrix such that the continuous closed-loop system*

$$\dot{x} = (A + BK)x \tag{2.5}$$

with $A \in \mathbb{R}^{nxn}$ and $B \in \mathbb{R}^{nxm}$ is asymptotically stable. Then the standard Lyapunov LMI problem to make such guarantee is defined as (see Zhou et al. (1996)) to find state-feedback matrix $K \in \mathbb{R}^{mxn}$ and a positive definite matrix $P \in \mathbb{R}^{nxn}$ such that

$$(A + BK)^{\intercal}P + P(A + BK) < 0. \tag{2.6}$$

Note that this problem is not linear due to the products between decision variables P and K. First, it is needed to apply a congruence transformation by multiplying both sides of each term in (2.6) *by $Q = P^{-1}$, obtaining*

$$QA^{\mathsf{T}} + AQ + QK^{\mathsf{T}}B^{\mathsf{T}} + BKQ < 0. \tag{2.7}$$

This new matrix inequality is still nonlinear due to the product between K and the new variable Q. A change of variable $L = KQ$ is then used to obtain

$$QA^{\mathsf{T}} + AQ + L^{\mathsf{T}}B^{\mathsf{T}} + BL < 0, \tag{2.8}$$

which is now an LMI with new variables $Q > 0$ and $L \in \mathbb{R}^{mxn}$. Finally, the state-feedback matrix K is found after solving (2.8) *by making $K = LQ^{-1}$. If it is also desirable, the Lyapunov matrix P can be found by making $P = Q^{-1}$.*

2.1.1.3 Schur Complement

Schur Complement is a tool used mainly to eliminate quadratic terms in matrix inequalities. The Schur Complement Lemma is stated as follows

Lemma 2.1.1 *Consider the following matrix inequality*

$$\begin{bmatrix} Q(x) & S(x) \\ S(x)^{\mathsf{T}} & R(x) \end{bmatrix} > 0, \tag{2.9}$$

where $Q(x) = Q(x)^{\mathsf{T}}$, $R(x) = R(x)^{\mathsf{T}}$, and $S(x)$ are matrices affine in x. Then the conditions

$$R(x) > 0 \text{ and } Q(x) - S(x)R(x)^{-1}S(x)^{\mathsf{T}} > 0 \tag{2.10}$$

are equivalent to (2.9)*.*

Example 2 illustrates the use of Lemma 2.1.1.

Example 2 *Consider the following matrix inequality*

$$\begin{bmatrix} AA^{\mathsf{T}} & 0 \\ 0 & \gamma^2 I \end{bmatrix} > 0. \tag{2.11}$$

where scalar $\gamma > 0 \in \mathbb{R}$ is the decision variable. The inequality in Equation 2.11 is not an LMI because of the quadratic term in γ. To rectify this, first divide Equation (2.11) *by* γ

$$\begin{bmatrix} A\frac{1}{\gamma}A^\intercal & 0 \\ 0 & \gamma I \end{bmatrix} > 0. \tag{2.12}$$

Then, rewrite Equation (2.12) *as follows*

$$\begin{bmatrix} 0 & 0 \\ 0 & \gamma I \end{bmatrix} - \begin{bmatrix} A \\ 0 \end{bmatrix} \begin{bmatrix} \frac{-1}{\gamma} \end{bmatrix} \begin{bmatrix} A^\intercal & 0 \end{bmatrix} > 0, \tag{2.13}$$

and use Lemma 2.1.1 to obtain the following LMI

$$\begin{bmatrix} 0 & 0 & A \\ 0 & \gamma I & 0 \\ A^\intercal & 0 & -\gamma I \end{bmatrix} > 0, \text{ with } \gamma > 0. \tag{2.14}$$

2.1.1.4 S-Procedure

The S-Procedure is a method that allows two or more inequalities to be combined into only one. This is specially useful when it is necessary to guarantee that a quadratic function is negative whenever other quadratic forms are positive (or negative).

Definition 2.1.2 *Let $F_0(x), ..., F_m(x)$ be quadratic functions of $x \in \mathbb{R}^n$ such as (BOYD et al., 1994)*

$$F_i(x) \triangleq x^\intercal A_i x + 2u_i^\intercal x + b_0, \text{ where } A_i = A_i^\intercal, i = 0, ..., m. \tag{2.15}$$

If there exist $\tau_1 \geq 0, ..., \tau_m \geq 0$ such that

$$\text{for all } x, F_0(x) - \sum_{i=1}^{m} \tau_i F_i(x) \geq 0, \tag{2.16}$$

then it holds that

$$F_0(x) \geq 0 \text{ for all } x \text{ such that } F_i(x) \geq 0 \tag{2.17}$$

Example 3 *Suppose that the following constraints on P and W hold, where* $x = \begin{bmatrix} x_1^\intercal & x_2^\intercal \end{bmatrix}^\intercal$,

$$x^\intercal \begin{bmatrix} A^\intercal P + P^\intercal A & PB \\ \star & 0 \end{bmatrix} x < 0 \tag{2.18}$$

$$x^\intercal \begin{bmatrix} 0 & -CW \\ \star & -2W \end{bmatrix} x \geq 0 \tag{2.19}$$

Then, by applying Definition 2.1.2, inequalities Equations (2.18) *and* (2.19) *can be combined into a single inequality as*

$$x^\intercal \begin{bmatrix} A^\intercal P + P^\intercal A & PB - CW\tau \\ \star & -2W\tau \end{bmatrix} x < 0, \text{ with } \quad \tau > 0. \tag{2.20}$$

Since τ *only appears adjacent to W, it is possible to apply the change of variable* $W\tau = V$. *Thus, the following LMI in* $P > 0$ *and* $V > 0$ *is obtained*

$$\begin{bmatrix} A^\intercal P + P^\intercal A & PB - CV \\ \star & -2V \end{bmatrix} < 0. \tag{2.21}$$

2.2 Lyapunov Stability of Discrete-Time Linear Systems

In this Section the fundamentals for stability analysis of the SDTC are constructed. As it will be demonstrated in Chapter 4, stability of the closed-loop system in the nominal case (when there are no uncertainties in the process model) depends upon the process fast-model. Thus, the Lyapunov criterion for the stability of systems without delay is reviewed in Subsection 2.2.1.

For robust stability analysis the process delay is not compensated by the predictor, and appears in the states of the equivalent closed-loop system. There exist two main methods to study stability of systems with delayed states, namely the Krasovskii and the Razumikhin methods of Lyapunov functionals (SUN; CHEN, 2017; FRIDMAN, 2014b). The former is the most popular, being applicable in a wider range of problems and leading to less conservative results (FRIDMAN, 2014a). Thus, it was the choice for this work and is reviewed in Subsection 2.2.2.

2.2.1 Stability of Systems without Delay

There are different forms of stability, being input-output stability and stability of equilibrium points the most used. The latter, which is used in this work, is characterized in the sense of Lyapunov functionals. An asymptotically stable equilibrium point is a point for which the trajectories of states with different initial conditions converge as time approaches infinity (KHALIL, 2002). The region of attraction of an equilibrium point x^* is the set of initial conditions x_0 for which $x(x_0,t) \to x^*$ as t goes to infinity (BRIAT, 2015). Furthermore, an equilibrium point is said to be globally stable if its region of attraction is the whole space, e.g. $\mathbb{R}^n$. Note that in the discrete-time domain, the time t dependence is usually replaced by the sample k.

In order to establish the stability of discrete-time linear systems without delay, the following Lyapunov condition is given

Theorem 2.2.1 *For a chosen positive definite function $V(x(k)) = x^T(k)Px(k)$, $\forall x \neq 0$, the discrete-time system $x(k+1) = f(x(k))$ is stable if and only if*

$$\Delta V(x(k)) \triangleq V(x(k+1)) - V(x(k)) < 0, \text{ with } P = P^{\mathsf{T}} > 0. \tag{2.22}$$

Note that Theorem 2.2.1 is in the form of a feasibility problem. It states that if there can be found any positive definite symmetric matrix P for which $\Delta V(x(k)) < 0$ holds, then the system $x(k+1) = f(x(k))$ is stable. This kind of problem can usually be solved in a very strait manner by using LMIs. The stability phenomena is illustrated in the example that follows.

Example 4 *Consider the following second-order discrete-time system*

$$x(k+1) = \begin{bmatrix} 2 & 0 \\ 1 & 3 \end{bmatrix} x(k) + \begin{bmatrix} 1 \\ 1 \end{bmatrix} u(k). \tag{2.23}$$

From classical control systems theory, the open-loop is unstable since the eigenvalues of A (3 and 2) are outside the unit circle. Consider then the problem of finding a stabilizing state feedback control law $u(t) = -Kx$; this substitution leads to the following equivalent closed-loop system

$$x(k+1) = (A - BK)x(k). \tag{2.24}$$

First, apply theorem 2.2.1 to Equation (2.24) *as follows*

$$V(x(k+1)) - V(x(k)) = x(k)^{\intercal}(A-BK)^{\intercal}P(A-BK)x(k) - x(k)^{\intercal}Px(k) > 0,\ P > 0. \tag{2.25}$$

Then, by rearranging (2.25) *one obtains*

$$x(k)^{\intercal}\left[(A-BK)^{\intercal}P(A-BK) - P\right]x(k) < 0,\ P > 0, \tag{2.26}$$

which is equivalent to simply

$$\left[(A-BK)^{\intercal}P(A-BK) - P\right] < 0,\ P > 0. \tag{2.27}$$

Next, apply the Schur complement Lemma to (2.27) *to obtain*

$$\begin{bmatrix} -P & A^{\intercal}+K^{\intercal}B^{\intercal} \\ \star & -P^{-1} \end{bmatrix} < 0,\ P > 0. \tag{2.28}$$

By applying a congruence transformation with $diag(P^{-1}, I)$*, and making the change of variable* $Q = P^{-1}$ *it is obtained*

$$\begin{bmatrix} -Q & QA^{\intercal}+QK^{\intercal}B^{\intercal} \\ \star & -Q \end{bmatrix} < 0,\ Q > 0. \tag{2.29}$$

Finally, by setting $K = NQ^{-1}$ *one obtains the following LMI.*

$$\begin{bmatrix} -Q & QA^{\intercal}+N^{\intercal}B^{\intercal} \\ \star & -Q \end{bmatrix} < 0,\ Q > 0. \tag{2.30}$$

Next, consider that the LMI in Equation (2.30) *was solved and the stabilizing state-feedback gain* $K = \begin{bmatrix} -0.93 & 2.97 \end{bmatrix}$ *was found. Closed-loop system* (2.24) *is now asymptotically stable with globally stable equilibrium point* $x^* = 0$*, i.e.* $\forall\, x_0 \in \mathbb{R}^2,\ x(x_0,k) \to x^*$ *as* $k \to \inf$*, since the eigenvalues of* $(A-BK)$ *(0.3 and 0.8) are inside the unit circle. Figure 3 illustrates a plot of part of the region of attraction using different initial conditions for states* x_1 *and* x_2*. Since the system is globally asymptotically stable, the region of attraction is the whole* $\mathbb{R}^2$ *space. The time response is shown in Figure 4. The effects of actuator saturation in the stability of such system will be shown in the second part of this example, in Section 2.3.*

Figure 3 – Convergent trajectories for equilibrium point in Example 4. Equilibrium point ($x^* = 0$); initial conditions (o).

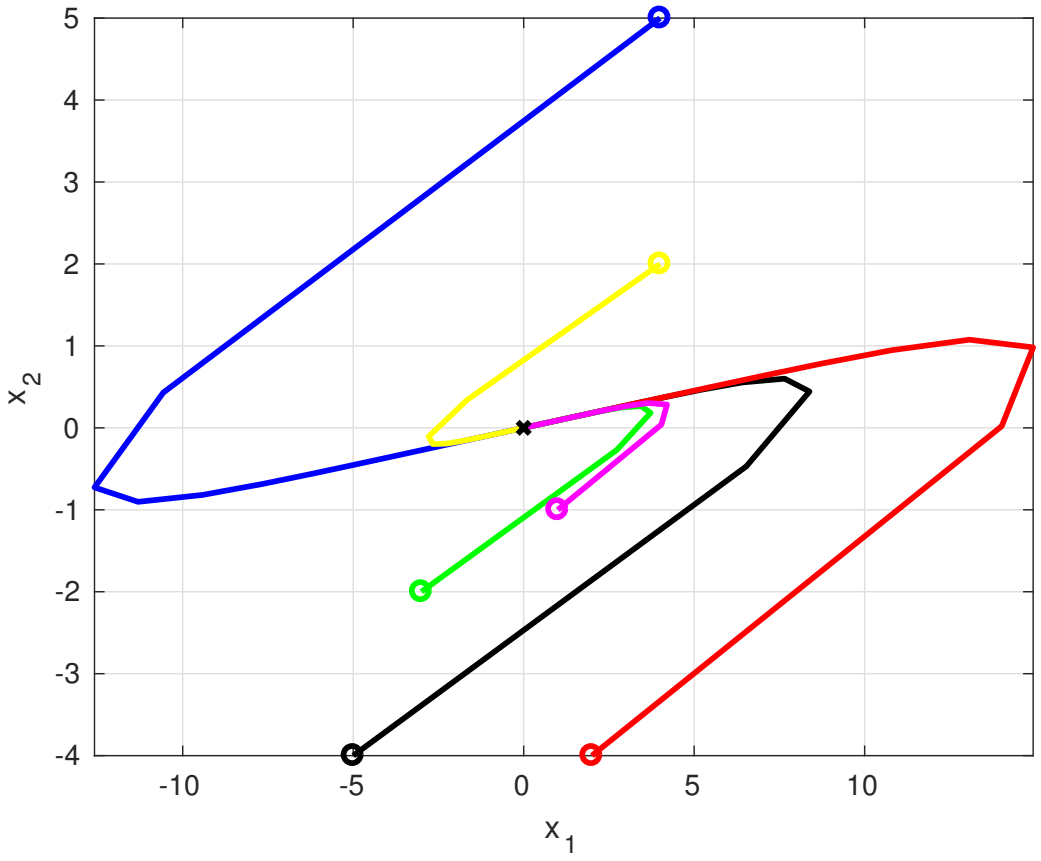

Source: The author.

2.2.2 Delay-Dependent Stability

In this Subsection, bases for the stability investigation of the SDTC with model uncertainties are established. As it will be seen in Chapter 4, the equivalent state-space closed-loop representation of the SDTC in the presence of model uncertainties is a system with delayed states. Furthermore, the delay in the states is equal to the delay of the process model. In this work, the delay in the controlled process is considered to be not only uncertain but also possibly time-varying.

As explained in the introductory chapter of this thesis, the motivation for the study of stability in the case of time-varying delays lies on the recent advance of networked controlled systems. Although NCSs are useful in a wide variety of applications, these systems introduced a robustness problem which is called *quenching phenomenon* in the literature (PAPACHRISTODOULOU *et al.*, 2007; LOUISELL, 2001). Basically, this phenomenon occurs when dead-time processes are stable for the case of constant delays but become unstable for

Figure 4 – Example 4 - time responses for six different initial conditions x_0.

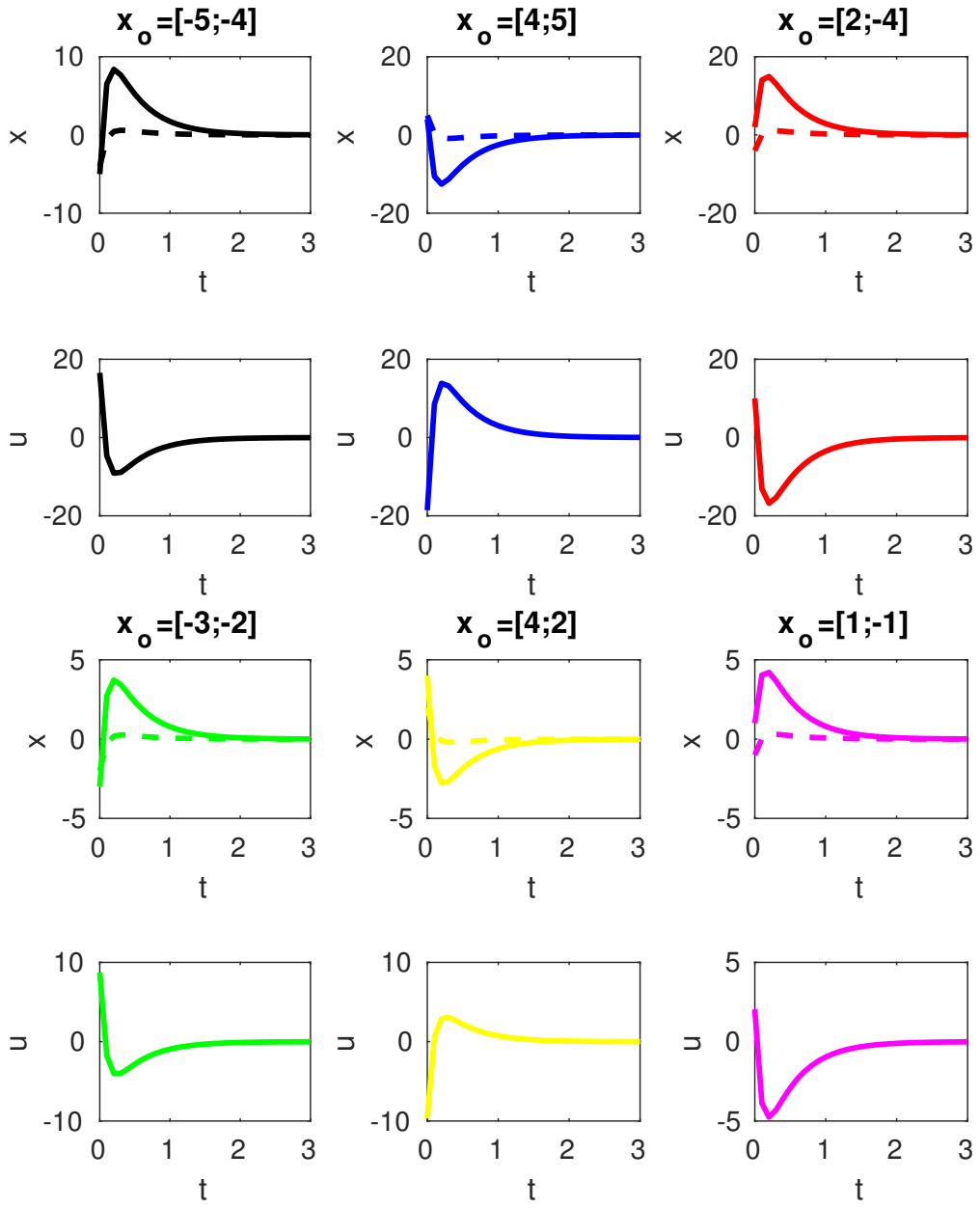

Source: The author.

time-varying ones, thus showing that the latter case is more harmful for the stability of control systems.

2.2.2.1 Lyapunov-Krasovskii Method

Consider the following discrete-time linear system with time-varying delay

$$x(k+1) = Ax(k) + A_d x(k-\tau_k),\ k \in \mathbb{Z}^+,\ \tau_k \in \mathbb{N},\ 0 \leq \tau_k \leq h_1. \tag{2.31}$$

For simplicity, denote $x_k(j) \triangleq x(k+j),\ j = -h_1, ..., 0$. When $\tau_k = h_1$ (worst case), the initial condition for (2.31) should be given as

$$col\{x(0), x(-1), ..., x(-h)\} = col\{\phi(0), \phi(-1), ..., \phi(-h)\}. \tag{2.32}$$

Then, consider the following Lemma borrowed from Fridman (2014a).

Lemma 2.2.1 *If there exist positive numbers* α, β *and a functional* $V : \underbrace{\mathbb{R}^n \times \ldots \times \mathbb{R}^n}_{h_1+1\ times} \to \mathbb{R}^+$ *such that for all* $k = 0, 1, 2 \ldots$

$$0 \leq V(x_k) \leq \beta\{max_{j\in[-h,0]}|x(k+j)|^2\} \tag{2.33}$$

and

$$V(x_{k+1}) - V(x_k) \leq -\alpha|x(k)|^2 \tag{2.34}$$

for $x(k)$ *satisfying* (2.31)*, then* (2.31) *is asymptotically stable.*

Proof of Lemma 2.33 comes directly from Fridman (2014a), page 248, and is shown in the sequence. From (2.34) it follows that

$$\sum_{j=0}^{k} V(x_{j+1}) - V(x_j) \equiv V(x_{k+1}) - V(x_0) \leq -\alpha \sum_{j=0}^{k} |x(j)|^2. \tag{2.35}$$

Then, due to (2.33), for $x(k)$ satisfying both (2.31) and (2.32), it is obtained that

$$|x(k)|^2 \leq \sum_{j=0}^{k} |x(j)|^2 \leq \frac{1}{\alpha} V(x_0) \leq \frac{\beta}{\alpha} \max_{j\in[-h,0]} |\phi(j)|^2, \quad \forall k \in \mathbb{Z}^+, \tag{2.36}$$

which implies that $|x(k)|^2$ is small for small enough $\max_{j\in[-h,0]}|\phi(j)|^2$. Furthermore,

$$\sum_{j=0}^{\inf}|x(j)|^2 \leq \frac{1}{\alpha}V(x_0) < \inf. \tag{2.37}$$

Hence, $|x(j)|^2 \to 0$ for $j \to \inf$, and the proof is complete.

Thus, the problem of providing stability proof for systems with delayed states can also be solved by choosing an appropriate Lyapunov functional $V(x)$, as stated by Lemma 2.2.1. Note that this condition is sufficient only, meaning that the choice of functional and its consequent manipulation can lead to more or less conservative results. This is a hot field of research, with many works published in the last ten years. For more details, see the works of Zhu and Yang (2008), Zhang *et al.* (2008), Shao and Han (2011), Liu and Zhang (2012) and Seuret *et al.* (2015).

In this work, some precautions are taken in order to yield less conservative results, such as employing the convex analysis of Park *et al.* (2011) and the *descriptor model transformation*, introduced in Fridman (2001). The *descriptor model transformation* makes it possible to analyze systems with fast-varying delays. The employment of the convex analysis approach will be exemplified in the derivation of stability results, whereas the discrete-time model transformation from Fridman (2014a) is reviewed in the following text.

2.2.2.1.1 Discrete-Time Descriptor System Review

The introduction of the descriptor method was mainly motivated by the conservatism of prior results in time-varying delay systems. The first Lyapunov-Krasovskii conditions dealt mainly with the case of slow-varying delays, while systems with fast-varying delays had to be analyzed by using system augmentation, i.e. delay-independent conditions in the form of Lyapunov-Razumikihn functionals. Consider the definition

$$\bar{y} = x(k+1) - x(k), \quad x(k+1) = \bar{y} - x(k). \tag{2.38}$$

Then it is clear that

$$x(k+1) - x(k) - \bar{y} = 0. \tag{2.39}$$

In order to illustrate the use of the descriptor method, first consider the case of a delay-free autonomous system given by

$$x(k+1) = Ax(k), \tag{2.40}$$

then substitute (2.40) into (2.39) to obtain

$$(A-I)x(k) - \bar{y} = 0, \tag{2.41}$$

which is equivalent to (2.40) in the sense of stability (FRIDMAN, 2014a). Consider the Lyapunov functional for stability of discrete-time systems without delay presented in Theorem 2.2.1. In the descriptor approach, $x(k+1) = \bar{y} - x(k)$ is substituted into $\Delta V(x(k))$ rather than the right-hand side of (2.31), thus

$$\Delta V(x(k)) = 2x^{\mathsf{T}}(k)P\bar{y}(k) + \bar{y}^{\mathsf{T}}(k)P\bar{y}(k). \tag{2.42}$$

Now, by using (2.41), it is clear that the following equation holds for free matrices P_2 and P_3

$$2[x^{\mathsf{T}}(k)P_2^{\mathsf{T}} + \bar{y}^{\mathsf{T}}(k)P_3^{\mathsf{T}}][(A-I)x(k) - \bar{y}] = 0. \tag{2.43}$$

Then, a new stability condition by using the descriptor method is found by adding (2.42) to (2.43), yielding

$$\Delta V(x(k)) + 2[x^{\mathsf{T}}(k)P_2^{\mathsf{T}} + \bar{y}^{\mathsf{T}}(k)P_3^{\mathsf{T}}][(A-I)x(k) - \bar{y}] < 0. \tag{2.44}$$

By substitution of (2.42) into (2.44), it follows that

$$2x^{\mathsf{T}}(k)P\bar{y}(k) + \bar{y}^{\mathsf{T}}(k)P\bar{y}(k) + 2[x^{\mathsf{T}}(k)P_2^{\mathsf{T}} + \bar{y}^{\mathsf{T}}(k)P_3^{\mathsf{T}}][(A-I)x(k) - \bar{y}] < 0, \tag{2.45}$$

which can be written in the LMI format as

$$\begin{bmatrix} P_2^{\mathsf{T}}(A-I) + (A-I)^{\mathsf{T}}P_2 & P - P_2^{\mathsf{T}} + (A-I)^{\mathsf{T}}P_3 \\ \star & P - P_3 - P_3^{\mathsf{T}} \end{bmatrix} < 0. \tag{2.46}$$

Then, the autonomous system (2.40) is asymptotically stable if there exist matrices $P > 0$, P_2 and P_3 such that (2.46) is feasible. This method will be used in this work instead of the traditional method where $x(k+1)$ is substituted into the Lyapunov functional. The two main advantages of using this method are described in Fridman (2014a) as

- The use of the descriptor method yields less conservative stability conditions (with or without delay).
- LMIs are easily extended for the case of uncertain systems, due to the affine relationship in the system matrices.

2.2.2.1.2 Interval Time-Varying Delay

Note that system (2.31) was defined for small like delays $\tau_k \in [0, h_1]$. However, the motivation in this work is to provide stability analysis for systems with non-small interval delays such as

$$x(k+1) = Ax(k) + A_d x(k-\tau_k),\ k \in \mathbb{Z}^+,\ \tau_k \in \mathbb{N},\ h_0 \leq \tau_k \leq h_1. \tag{2.47}$$

This can be achieved by considering the following Lyapunov-Krasovskii functional (FRIDMAN, 2014a)

$$V(x(k)) = V_P(k) + V_S(k) + V_R(k) + V_{S1}(k) + V_{R1}(k) \tag{2.48}$$

where

$$\begin{aligned}
V_P(k) &= x^T P x \\
V_S(k) &= \sum_{j=k-h_0}^{k-1} x^T(j) S x(j) \\
V_R(k) &= h_0 \sum_{m=-h_0}^{-1} \sum_{j=k+m}^{k-1} \overline{y}^T(j) R \overline{y}(j) \\
V_{S1}(k) &= \sum_{j=k-h_1}^{k-h_0-1} x^T(j) S_1 x(j) \\
V_{R1}(k) &= (h_1 - h_0) \sum_{m=-h_1}^{-h_0-1} \sum_{j=k+m}^{k-1} \overline{y}^T(j) R_1 \overline{y}(j) \\
\overline{y}(j) &= x(j+1) - x(j) \\
P > 0, S > 0, R > 0, S_1 > 0, R_1 > 0.
\end{aligned} \tag{2.49}$$

This analysis employs the discrete-time version of the Jensen's inequality (HIEN; TRINH, 2016), which is stated in the following Lemma.

Lemma 2.2.2 *For integers $a < b$, a function $\theta : \mathbb{Z}[a,b] \to \mathbb{R}^n$ and a matrix $R > 0$, the following inequality holds*

$$\sum_{k=a}^{b} \theta^{\intercal}(k) R \theta(k) \geq \frac{1}{l} \left(\sum_{k=a}^{b} \theta^{\intercal}(k) \right) R \left(\sum_{k=a}^{b} \theta(k) \right), \tag{2.50}$$

where $l = b - a + 1$ denotes the length of interval $[a,b]$ in $\mathbb{Z}$.

In order to find an LMI that establishes stability conditions for system in (2.47), it is necessary to find $\Delta V(x(k))$ as defined by Lyapunov functional in (2.48), (2.49). Thus, by applying suitable math to (2.49) and using the descriptor method substitution from Equation (2.38) it is found that

$$\Delta V_P(k) = 2x^T(k) P \overline{y}(k) + \overline{y}^T(k) P \overline{y}(k) \tag{2.51}$$

$$\Delta V_S(k) = x^T(k) S x(k) - x^T(k-h_0) S x(k-h_0) \tag{2.52}$$

$$\Delta V_{S1}(k) = x^T(k-h_0) S_1 x(k-h_0) - x^T(k-h_1) S x(k-h_1) \tag{2.53}$$

$$\Delta V_R(k) = h_0^2 \overline{y}^T(k) R \overline{y}(k) - h_0 \sum_{j=k-h_0}^{k-1} \overline{y}^T(j) R \overline{y}(j) \tag{2.54}$$

$$\Delta V_{R1}(k) = (h_1 - h_0)^2 \overline{y}^T(k) R_1 \overline{y}(k) - (h_1 - h_0) \sum_{j=k-h_1}^{k-h_0-1} \overline{y}^T(j) R_1 \overline{y}(j) \tag{2.55}$$

By applying Jensen's inequality to the summation terms in the right-hand side of equations (2.54) and (2.55), and using the reciprocally convex approach, the following relations are obtained

$$\Delta V_{R_{jen}}(k) \equiv h_0^2 \overline{y}^T(k) R \overline{y}(k) - [x^T(k) - x^T(k-h_0)] R [x(k) - x(k-h_0)] \geq \Delta V_R(k), \text{ and} \tag{2.56}$$

$$\Delta V_{R1_{jen}}(k) \equiv (h_1 - h_0)^2 \bar{y}^T(k) R_1 \bar{y}(k) - \eta^T \begin{bmatrix} R_1 & S_{12} \\ \star & R_1 \end{bmatrix} \eta \geq \Delta V_{R1}(k), \tag{2.57}$$

where

$$\eta = \begin{bmatrix} x(k-h_0) - x(k-\tau_k) \\ x(k-\tau_k) - x(k-h_1) \end{bmatrix}, \text{ and} \tag{2.58}$$

$$\begin{bmatrix} R_1 & S_{12} \\ \star & R_1 \end{bmatrix} \geq 0 \text{ for some } S_{12}. \tag{2.59}$$

Then, define

$$\Delta V_{time}(x(k)) = \Delta V_P(k) + \Delta V_S(k) + \Delta V_{S1}(k) + \Delta V_{R_{jen}}(k) + \Delta V_{R1_{jen}}(k), \tag{2.60}$$

which is computed as the sum of the terms in the right-hand side of equations (2.51), (2.52), (2.53), (2.56) and (2.57). Next, by applying the descriptor method to system (2.47), it is obtained

$$DESC_{uns}(k) \equiv 2[x^\intercal(k) P_2^\intercal + \bar{y}^\intercal(k) P_3^\intercal][(A-I)x(k) + A_d x(k) - \bar{y}] = 0. \tag{2.61}$$

Finally, by addition of (2.61) to (2.60) and definition of

$$\eta_{case_1}(k) = col\{x(k), \bar{y}(k), x(k-h_0), x(k-h_1), x(k-\tau_k)\}, \tag{2.62}$$

it is obtained that

$$V(x(k-1)) - V(x(k)) \leq \eta_{case_1}(k)^T \Upsilon_{11} \eta_{case_1}(k) \leq -\alpha |x(k)|^2, \tag{2.63}$$

is satisfied for some $\alpha > 0$, where Υ_{11} is defined in the following Theorem which establishes stability of system (2.47) in the case of time-varying delay.

Theorem 2.2.2 *The closed-loop system* (2.47) *is asymptotically stable for all time-varying delays* $h_0 \leq \tau_k \leq h_1$ *if there exist matrices* $P > 0, R > 0, S > 0, R_1 > 0, S_1 > 0, P_2, P_3, S_{12}$ *such that LMIs* (2.59) *and*

$$\Upsilon_{11} = \begin{bmatrix} \Psi_{11} & \Psi_{12} & R & 0 & P_2^T A_d \\ \star & \Psi_{22} & 0 & 0 & P_3^T A_d \\ \star & \star & \Psi_{33} & S_{12} & R - S_{12} \\ \star & \star & \star & \Psi_{44} & R_1 - S_{12}^T \\ \star & \star & \star & \star & \Psi_{55} \end{bmatrix} \leq 0 \tag{2.64}$$

are feasible, where

$$\begin{aligned} \Psi_{11} &= S - R + (A^T - I)P_2 + P_2^T(A - I), \\ \Psi_{12} &= P - P_2^T + (A^T - I)P_3, \\ \Psi_{22} &= P + Rh_0^2 + R_1(h_1 - h_0)^2 - P_3^T - P_3, \\ \Psi_{33} &= -R - S + S_1 - R_1, \\ \Psi_{44} &= -S1 - R1, \\ \Psi_{55} &= S_{12} + S_{12}^T - 2R_1. \end{aligned} \tag{2.65}$$

2.2.3 Robust Stability with Model Uncertainties

Model uncertainties are the differences between the actual system and its model. The less sensitive to such differences the more robust the control system is. In this Subsection, the LMI (2.64) is extended to the case of model uncertainties, which can be either structured (using polytopic representation) or unstructured (with norm-bounded matrices). Since the LMI (2.64) is affine in the system matrices, it can be applied to both of these cases.

2.2.3.1 Polytopic uncertainty

Structured uncertainties can be modeled as polytopic uncertainties when parameters in a transfer function or in a state-space matrix are unknown but bounded with known limits. A polytope is a convex hull which can represent structured uncertainties in systems, where each vertice is a combination of the known parameter limits.

Lets denote matrices A and A_d from system (2.47) with (FRIDMAN, 2014a)

$$\Gamma = \begin{bmatrix} A & A_d \end{bmatrix}, \quad \Gamma \in \Pi\{\Gamma_j, j = 1, ..., M\} \tag{2.66}$$

$$\Gamma = \sum_{j=1}^{M} \omega_j \Gamma_j, \quad \text{for some } 0 \leq \omega_j \leq 1, \sum_{j=1}^{M} \omega_j = 1, \tag{2.67}$$

where $\Gamma_j = \begin{bmatrix} A^j & A_d^j \end{bmatrix}$ describes the M vertices of the polytope. Then, the following corollary establishes stability of system (2.47) in the presence of polytopic like uncertainties.

Corollary 2.2.1 *Assume that* (2.59) *and M LMIs* (2.64) *written in the vertices of* Γ_j

$$\Upsilon_{11}^j = \begin{bmatrix} \Psi_{11}^j & \Psi_{12}^j & R & 0 & P_2^T A_d^j \\ \star & \Psi_{22} & 0 & 0 & P_3^T A_d^j \\ \star & \star & \Psi_{33} & S_{12} & R - S_{12} \\ \star & \star & \star & \Psi_{44} & R_1 - S_{12}^T \\ \star & \star & \star & \star & \Psi_{55} \end{bmatrix} \leq 0 \tag{2.68}$$

are feasible for the same matrices $P > 0, R > 0, S > 0, R_1 > 0, S_1 > 0, P_2, P_3$ *and* S_{12}*, where*

$$\begin{aligned} \Psi_{11}^j &= S - R + (A^{jT} - I)P_2 + P_2^T(A^j - I), \\ \Psi_{12}^j &= P - P_2^T + (A^{jT} - I)P_3. \end{aligned} \tag{2.69}$$

Then

$$\sum_{j=1}^{M} \omega_j \Upsilon_{11}^j = \Upsilon_{11} < 0, \tag{2.70}$$

and the closed-loop system (2.47) *with polytopic type uncertainties described by* (2.66) *and* (2.67) *is asymptotically stable for all time-varying delays* $h_0 \leq \tau_k \leq h_1$.

2.2.3.2 Norm-bounded uncertainty

Consider the following system

$$x(k+1) = [A + \Delta A(k)]x(k) + [A_d + \Delta A_d(k)]x(k - \tau_k), \tag{2.71}$$

where the norm-bounded uncertainties are of the form $\begin{bmatrix}\Delta A(k) & \Delta A_d(k)\end{bmatrix} = \overline{E}\delta(k)\begin{bmatrix}\overline{H_A} & \overline{H_{Ad}}\end{bmatrix}$. The matrices $\overline{E}$, $\overline{H_A}$ and $\overline{H_{Ad}}$ are constant and known, whereas $\delta(k)$ is an unknown time-varying matrix satisfying

$$\delta^T(k)\delta(k) \leq I. \tag{2.72}$$

In order to analyse this case, first matrices A and A_d are replaced in Υ_{11} (Equation (2.64)) by $A + \overline{E}\delta(k)\overline{H_A}$ and $A_d + \overline{E}\delta(k)\overline{H_{Ad}}$, respectively. Then, separation of terms with uncertainties leads to the following inequality

$$\Upsilon_{11} + \Upsilon_{12}\delta(k)\Upsilon_{13}^T + \Upsilon_{13}\delta(k)^T\Upsilon_{12}^T < 0. \tag{2.73}$$

where

$$\Upsilon_{12} = \begin{bmatrix} P_2^T\overline{E} \\ P_3^T\overline{E} \\ 0 \\ 0 \\ 0 \end{bmatrix}, \quad \Upsilon_{13} = \begin{bmatrix} \overline{H_A}^T \\ 0 \\ 0 \\ 0 \\ \overline{H_{Ad}}^T \end{bmatrix}. \tag{2.74}$$

Then, by the application of the following inequality for some scalar $\varepsilon > 0$ (XIE, 1996)

$$\Upsilon_{12}\delta(k)\Upsilon_{13}^T + \Upsilon_{13}\delta(k)^T\Upsilon_{12}^T \leq \varepsilon^{-1}\Upsilon_{12}\Upsilon_{12}^T + \varepsilon\Upsilon_{13}\Upsilon_{13}^T, \tag{2.75}$$

and Schur complements, the following LMI is obtained

$$\begin{bmatrix} \Upsilon_{11} & \Upsilon_{12} & \varepsilon\Upsilon_{13} \\ \star & -\varepsilon & 0 \\ \star & \star & -\varepsilon \end{bmatrix} < 0. \tag{2.76}$$

Then, the following Corollary establishes robust stability of system (2.71).

Corollary 2.2.2 *The system* (2.71) *is asymptotically stable for all time-varying delays* $h_0 \leq \tau_k \leq h_1$ *and all* $\delta(k)$ *satisfying Equation* (2.72) *if there exists matrices* $P > 0, R > 0, S > 0, R_1 > 0, S_1 > 0, P_2, P_3, S_{12}$ *and scalar* $\varepsilon > 0$ *such that LMIs* (2.76) *and* (2.59) *are feasible.*

2.3 Stability of Systems with Actuator Saturation

2.3.1 Fundamentals

Systems with saturating actuators are on the boundary between linearity and nonlinearity. Even if an open-loop process is linear, the saturation of the actuator will turn the closed-loop into a nonlinear system. Thus, in this Section, the basis for understanding how saturation affects stability and performance of closed-loop systems is briefly presented. The stability condition is presented using the sector nonlinearity model approach, whereas a performance condition is presented in the form of the $\mathscr{L}_2$ gain.

There are three main approaches to tackling the stability problem of saturating systems, namely the global, semi-global and regions of stability approaches. When saturation occurs, it may not be possible to guarantee asymptotic stability of the closed-loop system for all initials conditions. Determination of the so called *regions of stability* is, thus, of theoretical importance for analysis of such systems. Herein, the phenomena of loss of stability for different initial conditions is illustrated by means of Example 4. However, the problem of finding ellipsoids of stability is not treated further, as this thesis concentrates in providing global stability analysis only.

Example 5 *Consider the same second-order discrete-time open-loop unstable system from Example 4*

$$x(k+1) = A = \begin{bmatrix} 2 & 0 \\ 1 & 3 \end{bmatrix} x(k) + \begin{bmatrix} 1 \\ 1 \end{bmatrix} u(k) \tag{2.77}$$

Once again, consider a state feedback control law $u(k) = -Kx(k)$*, with* $K = \begin{bmatrix} -0.93 & 2.97 \end{bmatrix}$*. When saturation is absent, the linear closed-loop system is stable with eigenvalues 0.3 and 0.8, and is governed by the dynamics of Equation* (2.24)*. Convergent trajectories for different initial conditions were plotted in Example 4. Now, lets suppose that the control signal actually is saturated with boundaries* $-10 \leq u(k) \leq 10$*. Now, the closed-loop system is nonlinear with the*

form

$$x(k+1) = Ax(k) + Bsat(Kx(k)),\ with\ sat(Kx(k)) = \begin{cases} 10, & if\ Kx(k) > 10 \\ Kx(k), & if\ |Kx(k)| \leq 10 \\ -10, & if\ Kx(k) < -10 \end{cases} \tag{2.78}$$

Figures 5 and 6 show the trajectories and the time-response of the saturated system for the same initial conditions of Example 4. Note that now three of the trajectories were divergent, for $x_0 = [-5;-4]$, $x_0 = [4;5]$ *and* $x_0 = [2;-4]$. *In these cases, the system remained saturated for almost all the time. Interestingly, for both* $x_0 = [-3;-2]$ *and* $x_0 = [4;2]$, *spite of the control getting saturated in the initial instants, the trajectories converge for the origin. It is clear that, although being asymptotically stable to the origin in the absence of saturation, the origin becomes only a regional equilibrium point in the presence of the saturation nonlinearity.*

Figure 5 – Convergent and divergent trajectories in Example 5. Regional equilibrium point ($x^* = 0$); initial conditions (o).

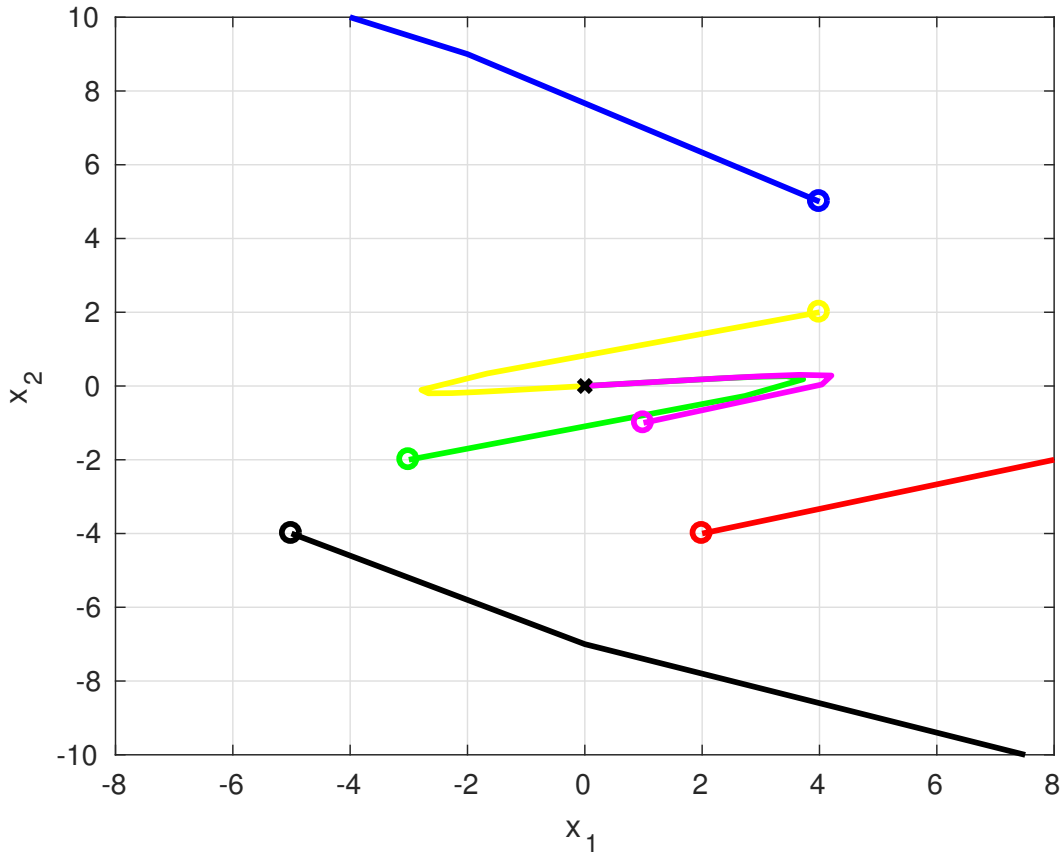

Source: The author.

Figure 6 – Example 5 - time responses for six different initial conditions.

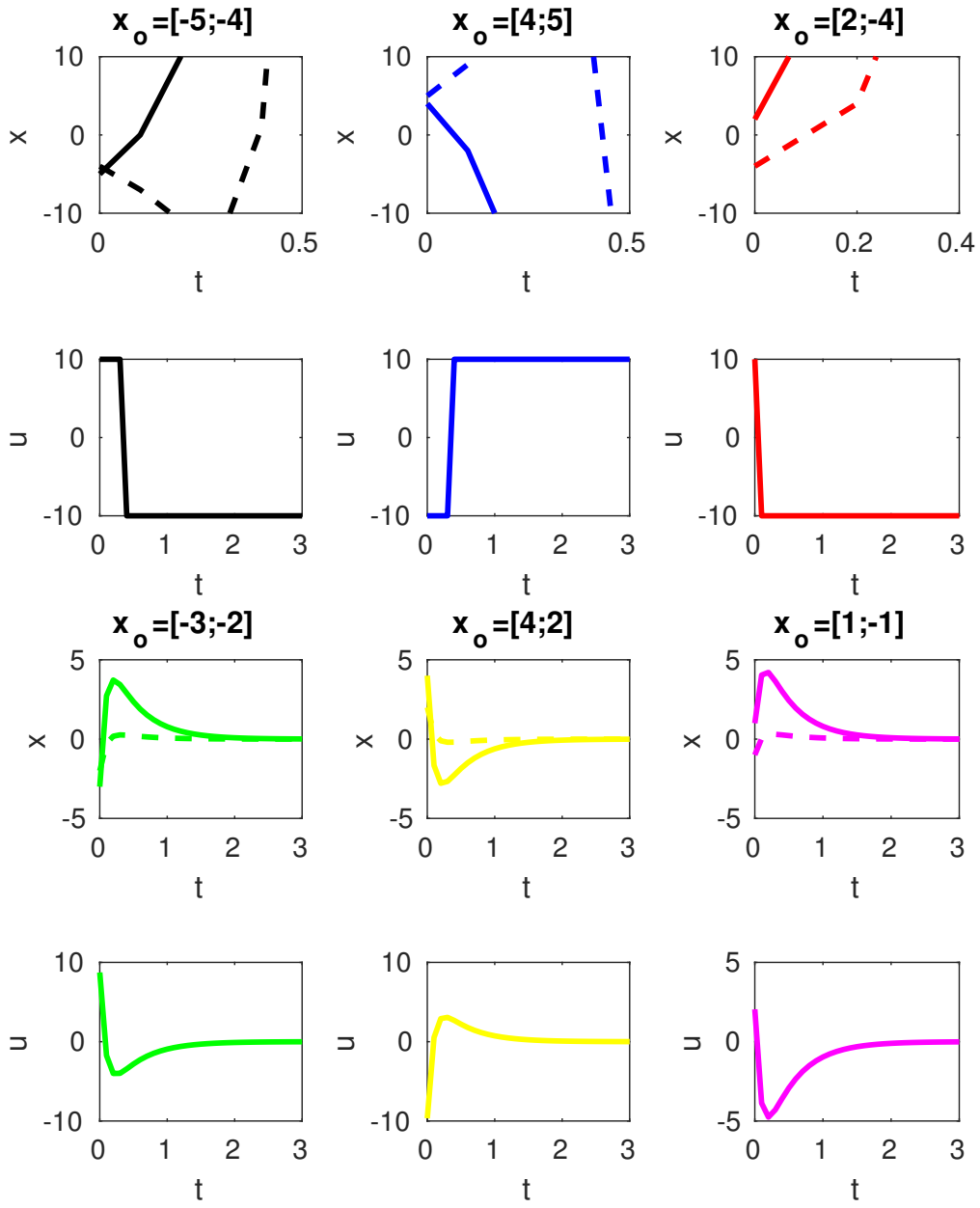

Source: The author.

2.3.2 Global Stabilization

One might wonder if it is possible to design a state-feedback control law for which system (2.77) is asymptotically stable for any saturation value. The answer to this question is a simple no, since it has been shown long ago that systems with unstable poles cannot be globally stabilized; see, for example Yang *et al.* (1997) for the case of discrete-time systems, from where

the following formal result can be stated

Theorem 2.3.1 *A discrete-time system*

$$x(k+1) = Ax(k) + Bu(k) \tag{2.79}$$

can only be globally stabilized by means of bounded feedback control laws if and only if
1. the pair (A,B) is stabilizable;
2. all the eigenvalues of matrix A have modulus equal to or less than 1,
where system (2.79) *is said to be globally asymptotically stabilizable if and only if there exists a bounded control law for which* $x^* = 0$ *is the global equilibrium point, i.e. for any initial condition* x_0*, the trajectory* $x(x_0,k) \to 0$ *as* $k \to \infty$*.*

Consider system (2.79) with a feedback control law $u(k) = -Kx(k)$ and lets formally define the saturation nonlinearity model for SISO systems (since this work does not treat the case of Multiple-input Multiple-output (MIMO) systems) as

$$sat(u) = sign(u) \times min\{|u|, |\bar{u}|\}, \bar{u} > 0, \tag{2.80}$$

Figure 7 – The saturation function.

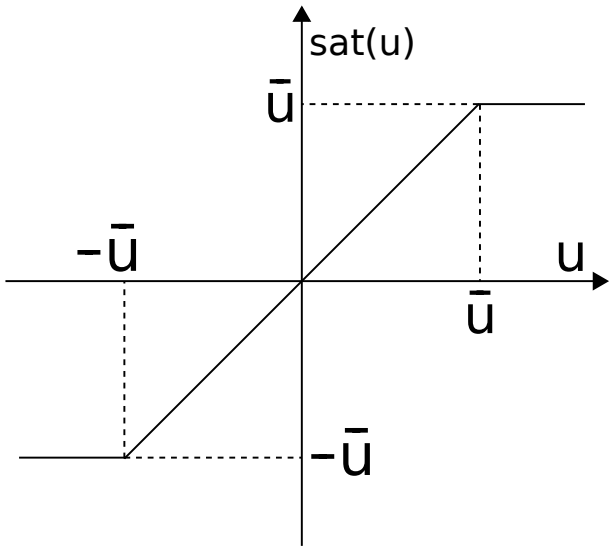

Source: The author.

where $\bar{u}$ is the bound on the control signal. Then, the closed-loop system can be re-written as

$$\begin{cases} x(k+1) = Ax(k) + Bsat(u(k)) \\ u(k) = -Kx(k). \end{cases} \tag{2.81}$$

This kind of representation, however, is not interesting for the study of stability, and the following dead-zone operator is defined

$$Dz(u) = u - sat(u), \tag{2.82}$$

thus closed-loop system (2.81) can be re-written in a equivalent manner as

$$\begin{cases} x(k+1) = [A+BK]x(k) + BDz(u(k)), \\ u(k) = -Kx(k), \end{cases} \tag{2.83}$$

Note that, when there is no saturation in the control signal $u(k) = sat(u(k)) = 0$, thus the problem of stability of (2.83) is reduced back to the problem of stability of system (2.79). Therefore, the connection between a linear system and the nonlinear operator Dz is clear.

Consider now the following equations

$$\begin{aligned} &\text{for } u \geq 0 : Dz(u) \geq 0 \text{ and } Dz(u) \leq \lambda u, \\ &\text{for } u \leq 0 : Dz(u) \leq 0 \text{ and } Dz(u) \geq \lambda u, \end{aligned} \tag{2.84}$$

where λ is a positive scalar. When $\lambda = 1$, the decentralized nonlinearity $Dz(u)$ is said to belong globally to $Sector[0,1]$. Similarly, when $\lambda < 1$ it is said that $Dz(u)$ belongs locally to $Sector[0,\lambda]$. This study focus on global stability, then from eq. (2.84) and for some one-by-one matrix $W > 0$, the following inequality holds

$$2Dz(u)^T W[u - Dz(u)] \geq 0. \tag{2.85}$$

LMIs that state the global stability condition for systems with input saturation can be derived by using a Lyapunov functional together with the sector condition presented in (2.85). This is illustrated in the following example.

Figure 8 – Dead-zone nonlinearity in the global sector.

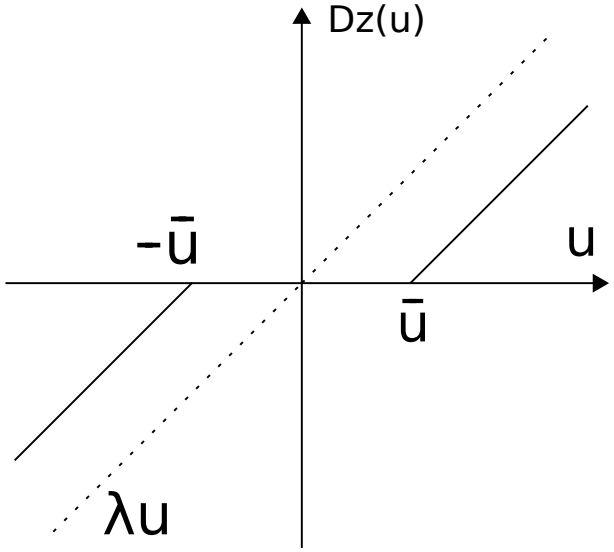

Source: The author.

Example 6 *Consider the problem of checking if the closed system* (2.83) *is globally stable for a given state-feedback matrix K. By denoting* $A_{cl} = A + BK$, $\tilde{u} = Dz(u)$, *and applying the Lyapunov functional from Theorem 2.2.1*

$$\Delta V(x(k)) = [x^{\intercal}(k)A_{cl}^{\intercal} + \tilde{u}^{\intercal}B^{\intercal}]P[A_{cl}x(k) + B\tilde{u}] - x(k)^{\intercal}Px(k) < 0, \tag{2.86}$$

which can be written in matrix form as

$$\begin{bmatrix} x(k) \\ \tilde{u}(k) \end{bmatrix}^{\intercal} \begin{bmatrix} A_{cl}^{\intercal}PA_{cl} - P & A_{cl}^{\intercal}PB \\ \star & B^{\intercal}PB \end{bmatrix} \begin{bmatrix} x(k) \\ \tilde{u}(k) \end{bmatrix} < 0. \tag{2.87}$$

Moreover, applying the sector boundedness condition (2.85) *to* (2.83)

$$2u(\tilde{k})W[-Kx(k) - \tilde{u}(k)] \geq 0, \tag{2.88}$$

which can be written in matrix format as

$$\begin{bmatrix} x(k) \\ \tilde{u}(k) \end{bmatrix}^{\intercal} \begin{bmatrix} 0 & -K^{\intercal}W \\ \star & -2W \end{bmatrix} \begin{bmatrix} x(k) \\ \tilde{u}(k) \end{bmatrix} \geq 0. \tag{2.89}$$

By using the S-procedure, inequalities (2.87) *and* (2.89) *can be combined as*

$$\begin{bmatrix} A_{cl}^{\intercal}PA_{cl} - P & A_{cl}^{\intercal}PB - K^{\intercal}W\tau \\ \star & B^{\intercal}PB - 2W\tau \end{bmatrix} < 0, \text{ for some } \tau > 0. \tag{2.90}$$

Since τ only appears adjacent to W, the change of variable $V = W\tau$ can be applied, thus

$$\begin{bmatrix} A_{cl}^{\intercal}PA_{cl} - P & A_{cl}^{\intercal}PB - K^{\intercal}V \\ \star & B^{\intercal}PB - 2V \end{bmatrix} < 0. \tag{2.91}$$

Finally, closed-loop system (2.83) *is globally asymptotically stable if LMI* (2.91) *is feasible for some $P > 0$, $W > 0$. Note that, in this example, K was supposedly designed using conventional methods and is previously known, thus not being a decision variable in* (2.91)*. If the project of K was the intention, tough,* (2.91) *would need to be further manipulated. However, the use of LMIs in this work is concerned with demonstrating stability of closed-loops in the presence of actuator saturation (and also process delay) rather than synthesizing stabilizing control laws.*

In order to establish a performance indicator for the SDTC anti-windup strategy (in the nominal case) the following definition will be used throughout this work.

Definition 2.3.1 *A nonlinear system with input $u_{lin}(k)$ and output $y_d(k)$ has an $\mathscr{L}_2$ gain of γ when*

$$|y_d|_2 < \gamma|u_{lin}|_2 + \theta, \tag{2.92}$$

where $|.|_2$ denotes the standard Euclidean vector norm and θ is a positive constant.

The $\mathscr{L}_2$ gain represents a bound on the root mean square energy gain of a nonlinear system.

3 THE SIMPLIFIED DEAD-TIME COMPENSATOR

This Chapter presents the SDTC control structure and its tuning procedures. Initially, a review of the SDTC (TORRICO *et al.*, 2016) is presented in Section 3.1. Later, in Section 3.2, the anti-windup strategy for the SDTC (AWSDTC) is explained.

3.1 Review of the Simplified Dead-Time Compensator (SDTC)

The unsaturated SDTC control structure is depicted in Fig. 9, where $P_n(z) = G_n(z)z^{-d_n}$ is the nominal process, with $G_n(z)$ and d_n being the fast model and nominal dead-time, respectively. Plant $P(z) = G(z)z^{-\tau_k}$ is the model of the real process. The input-output transfer functions for the nominal case ($P_n(z) = P(z)$) are

$$H_{yr}(z) = \frac{Y(z)}{R_{ef}(z)} = \frac{K_r P_n(z)}{1 + R(z) + G_n(z)F(z)}, \tag{3.1}$$

$$H_{yq}(z) = \frac{Y(z)}{Q(z)} = P_n(z)\left[1 - \frac{P_n(z)V(z)}{1 + R(z) + G_n(z)F(z)}\right], \tag{3.2}$$

$$H_{un}(z) = \frac{U(z)}{N(z)} = \frac{-V(z)}{1 + R(z) + G_n(z)F(z)}, \tag{3.3}$$

where $U(z)$, $Y(z)$, $R_{ef}(z)$, $N(z)$ and $Q(z)$ refer to the Z-transform of the control action $u(k)$, process output $y(k)$, reference $r_{ef}(k)$, measurement noise $n(k)$, and input load disturbance $q(k)$, respectively.

For such control strategy, robust stability is achieved if the following condition

$$I_{\mathrm{r}}(\omega) = \frac{\mid 1 + R(e^{j\omega T_s}) + G_n(e^{j\omega T_s})F(e^{j\omega T_s}) \mid}{\mid G_{\mathrm{n}}(e^{j\omega T_s})V(e^{j\omega T_s}) \mid} > \overline{\delta P}(\omega), \tag{3.4}$$

is met, where T_s is the sampling time, $0 < \omega < \pi/T_s$, $\overline{\delta P}(j\omega)$ is the norm-bounded multiplicative uncertainty, and $I_r(\omega)$ is defined as robustness index.

It is important to highlight from Equations (3.1) to (3.4) that K_r, $R(z)$ and $F(z)$ can be tuned in order to obtain a desired set-point tracking, while the filter $V(z)$ is set for: (i) to cancel the effect of slow or unstable poles for disturbance rejection $H_{yq}(z)$; (ii) to obtain a desired trade-off between robustness and disturbance rejection.

Figure 9 – SDTC conceptual structure.

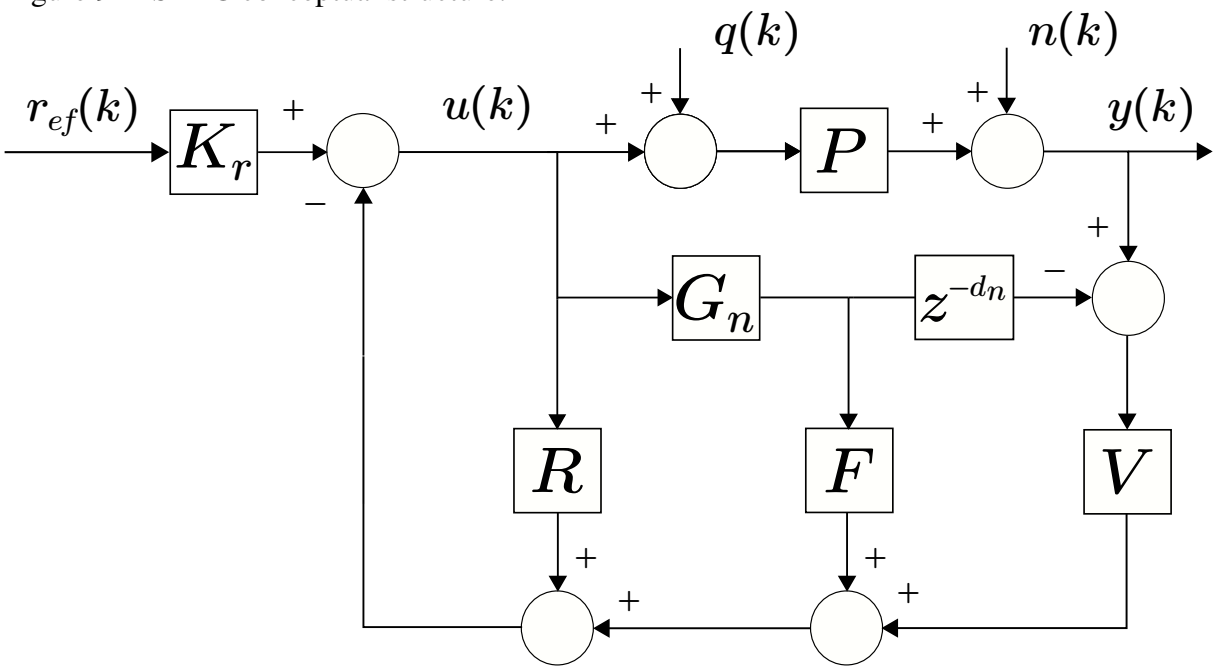

Source: The author.

3.1.1 Tuning of the primary controller

Simple tuning rules for the primary controller, defined by K_r, $R(z)$, and $F(z)$, were established by (TORRICO *et al.*, 2016) in order to obtain a desired set-point tracking. Feedback polynomials $R(z)$ and $F(z)$ are FIR filters

$$R(z) = r_1 z^{-1} + r_2 z^{-2} + ... + r_{n-1} z^{-n+1}, \tag{3.5}$$

$$F(z) = f_0 + f_1 z^{-1} + f_2 z^{-2} + ... + f_{n-1} z^{-n+1}, \tag{3.6}$$

where n is the order of the fast model $G_n(z)$. Coefficients of $R(z)$ and $F(z)$ are obtained by means of classical design techniques (such as pole allocation) in order to reach a desired set-point tracking response. This work uses the cited technique, thus the coefficients of R and F are found

by solving an equation of the type $Mx = y$, with

$$2n-1\left\{\begin{bmatrix} 1 & 0 & \dots & 0 & b_1 & \dots & 0 \\ a_1 & 1 & & \vdots & b_2 & & \vdots \\ \vdots & a_1 & & 0 & \vdots & & 0 \\ a_n & \vdots & & 1 & b_n & & b_1 \\ 0 & a_n & & a_1 & 0 & & \vdots \\ 0 & 0 & & a_n & 0 & & b_n \end{bmatrix}\right. \begin{bmatrix} r_1 \\ \vdots \\ r_{n-1} \\ f_0 \\ \vdots \\ f_{n-1} \end{bmatrix} = \begin{bmatrix} p_1 - a_1 \\ \vdots \\ p_n - a_n \\ p_{n+1} \\ \vdots \\ p_{2n-1} \end{bmatrix}, \tag{3.7}$$

$$\underbrace{\qquad\qquad}_{n-1} \quad \underbrace{\qquad}_{n}$$

where M is a non-singular $2n-1$ square matrix, $a_1 \dots a_n$ and $b_1 \dots b_n$ are the coefficients of

$$G_n(z) = \frac{b_1 z^{-1} + b_2 z^{-2} \dots b_n z^{-n}}{1 + a_1 z^{-1} + a_2 z^{-2} \dots a_n z^{-n}}, \tag{3.8}$$

and $p_1 \dots p_{2n-1}$ are the coefficients of the desired characteristic polynomial.

Note that in the case of FOPDT systems, $R(z) = 0$ and $F(z) = f_0$, which is a simple gain, thus the control structure reduces to the one presented in (TORRICO *et al.*, 2013). K_r is a gain calculated to yield zero steady-state error, then it follows that

$$K_r = \frac{1 + F_1(1) + G_n(1)F_2(1)}{P_n(1)}. \tag{3.9}$$

3.1.2 Tuning of the robustness filter $V(z)$

Robustness filter $V(z)$ is tuned aiming: (i) to reject step-like disturbances applied in the control signal; (ii) to eliminate slow modes of the plant model $P_n(z)$; (iii) to establish desired compromise between robustness and disturbance rejection. Such goals can be met by applying the following filter

$$V(z) = \frac{b_0 + b_1 z^{-1} + ... + b_p z^{-p}}{(1 - \beta z^{-1} 1)^{p+1}}, \tag{3.10}$$

where p is the number of slow modes of the plant model and β is the filter tuning parameter. For the first objective (i) $H_{yq}(z)$ must be zero at steady-state, i. e.

$$V(1) = \frac{1 + R(1) + G_n(1)F(1)}{P_n(1)}. \tag{3.11}$$

For the second objective (ii), the poles p_i of the process model must be canceled from $H_{yq}(z)$, thus

$$\left[1 - \frac{P_n(z)V(z)}{1 + R(z) + G_n(z)F(z)}\right]_{z=p_i \neq 1} = 0, \tag{3.12}$$

$$\frac{d}{dz}\left[1 - \frac{P_n(z)V(z)}{1 + R(z) + G_n(z)F(z)}\right]_{z=p_i=1} = 0. \tag{3.13}$$

Then, coefficients $b_0 \ldots b_p$ are computed using (3.11), (3.12) and (3.13). Such equations altogether set a linear system so that coefficients $b_0 \ldots b_p$ can be readily found.

Frequency response characteristics of the objective (iii) can be met by user adjustment of $0 < \beta < 1$ parameter.

3.2 The Anti-windup SDTC (AWSDTC)

It is an essential question for any anti-windup control strategy a proper knowledge of the control signal excursion in nominal operation. Within this context, it is fundamental to obtain the control law for the SDTC structure, which can be found by inspection on its block diagram presented in Figure 9, leading to

$$U(z) = \frac{K_r R_{ef}(z) - V(z)Y(z)}{1 + S(z)}, \tag{3.14}$$

where

$$S(z) = R(z) + G_n(z)(F(z) - V(z)z^{-d}) \tag{3.15}$$

is used to obtain an internally stable implementation of the SDTC for any process, as illustrated in Figure 10.

Figure 10 – SDTC implementation structure.

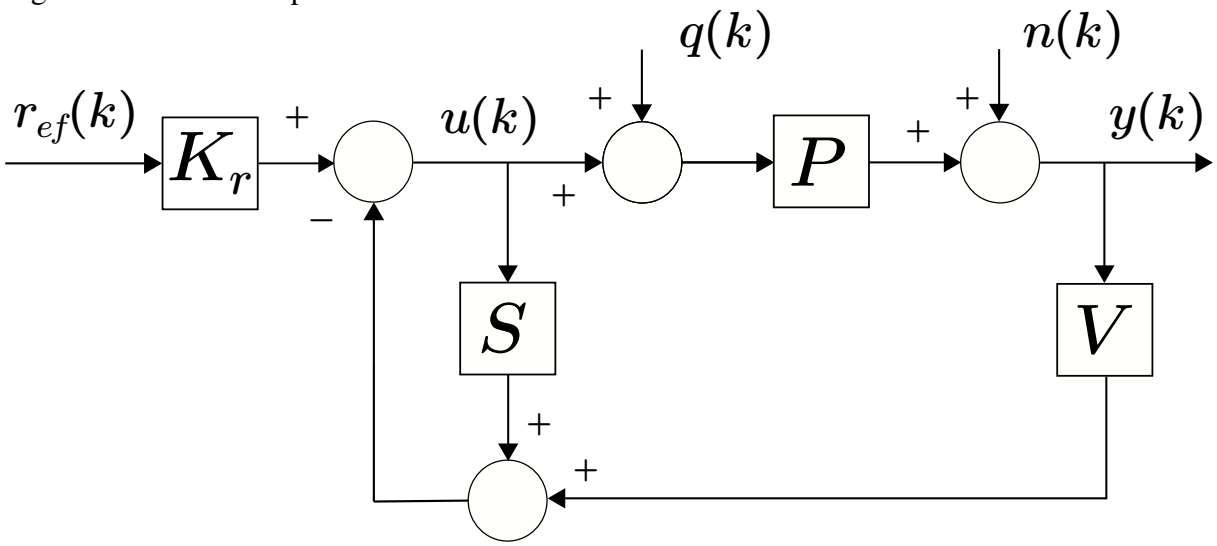

Source: The author.

Note that if the plant is under input saturation, the integrative and slow modes of $1+S(z)$ can produce the windup effect, leading the system to become oscillatory or even unstable.

Anti-windup characteristics of the SDTC is devised by simply adding the nonlinear saturation model

$$sat(u) = sign(u) \times min\{|u|, |\bar{u}|\}, \bar{u} > 0 \tag{3.16}$$

prior to the input of the plant, as illustrated in Figure 11.

Figure 11 – Anti-windup SDTC scheme.

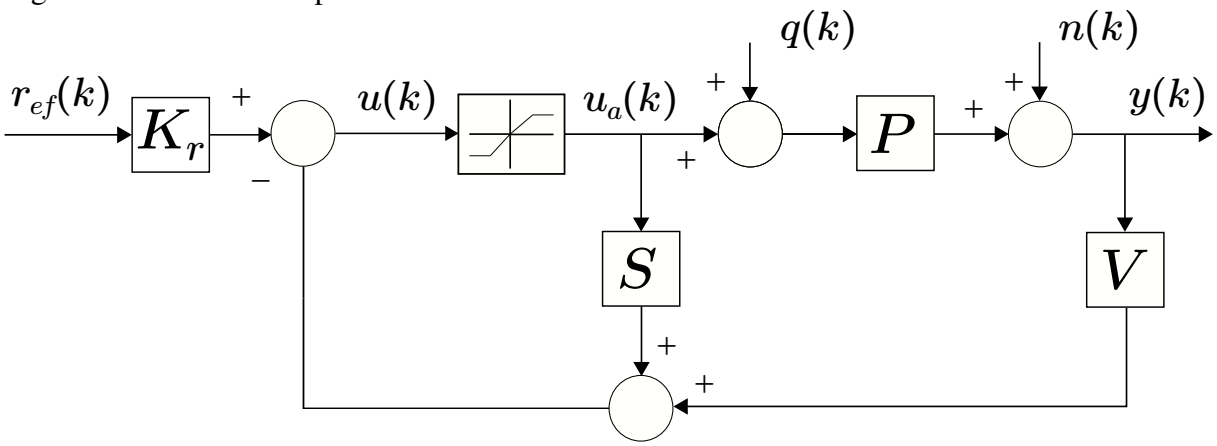

Source: The author.

In this case, the control signal is given by

$$U(z) = K_r R_{ef}(z) - (1 + S(z))U_a(z) - V(z)Y(z). \tag{3.17}$$

In order to properly analyze anti-windup characteristics of the SDTC controller, important features related to the reference tracking and disturbance rejection must be observed as following.

For such control strategy reference tracking is reached by means of K_r given in equation (3.9), which is a simple gain computed from steady-state behavior. On the other hand disturbance rejection is guaranteed by the proper design and tuning of the $V(z)$ robustness filter in equation (3.10).

Therefore, one may notice that neither K_r nor $V(z)$ apply integral action to accomplish control tasks. These features are the essentials which makes the SDTC useful to deal with saturation in control signal, as it never cumulatively integrates saturated values. Such observation can be easily noticed in equation (3.17).

4 CLOSED-LOOP STABILITY ANALYSIS

This Chapter presents global closed-loop stability analysis of the AWSDTC structures for both nominal (in Section 4.1) and modeling uncertainty (in Section 4.2) cases. Furthermore, Section 4.2 also presents robust stability results for the unsaturated SDTC. For organization purposes, the demonstration of some content used in Section 4.1 were moved to Appendix A.

Previous studies have proven that closed-loop global stability in the presence of actuator saturation cannot be achieved by a bounded input in the case of unstable processes (SONTAG, 1984), (LASSERRE, 1993) (also see Theorem 2.3.1). In case of critically stable processes, closed loop stability can only be achieved with nonlinear control laws (TARBOURIECH G. GARCIA, 2011).

Thus, in this thesis it is assumed that all the poles of the fast model $G_n(z)$ (for nominal stability analysis) are within the closed unit circle, and there are no multiple poles with $|z| = 1$. Also, it is assumed that the plant $P(z) = G(z)z^{-\tau_k}$ remains stable even in the presence of modeling uncertainties (for robust stability analysis). The theoretical background necessary to establish stability conditions of the AWSDTC were presented in Chapter 2. Note that in this work the control strategy is limited to SISO systems.

4.1 Nominal Stability Analysis of the AWSDTC

In order to analyse stability and performance of the nominal anti-windup SDTC ($P_n(z) = P(z)$), the scheme in Fig. 11 is redrawn in a more attractive equivalent form depicted by Fig. 12 (see **demonstration** in Appendix A), where

$$M_1(z) = \frac{G_n(z)}{1 + R(z) + G_n(z)F(z)}, \text{ and} \tag{4.1}$$

$$M_2(z) = -\frac{R(z) + G_n(z)F(z)}{1 + R(z) + G_n(z)F(z)}. \tag{4.2}$$

As it can be seen, the system is divided in three parts, namely the linear loop, the nonlinear loop and the disturbance filter, with output $y = y_{lin} - y_d z^{-d_n}$. This kind of decoupled structure is widely used for the purpose of stability analysis of closed-loop systems under input saturation (see Turner and Postlethwaite (2007) for instance).

Figure 12 – Equivalent Structure for Stability Analysis.

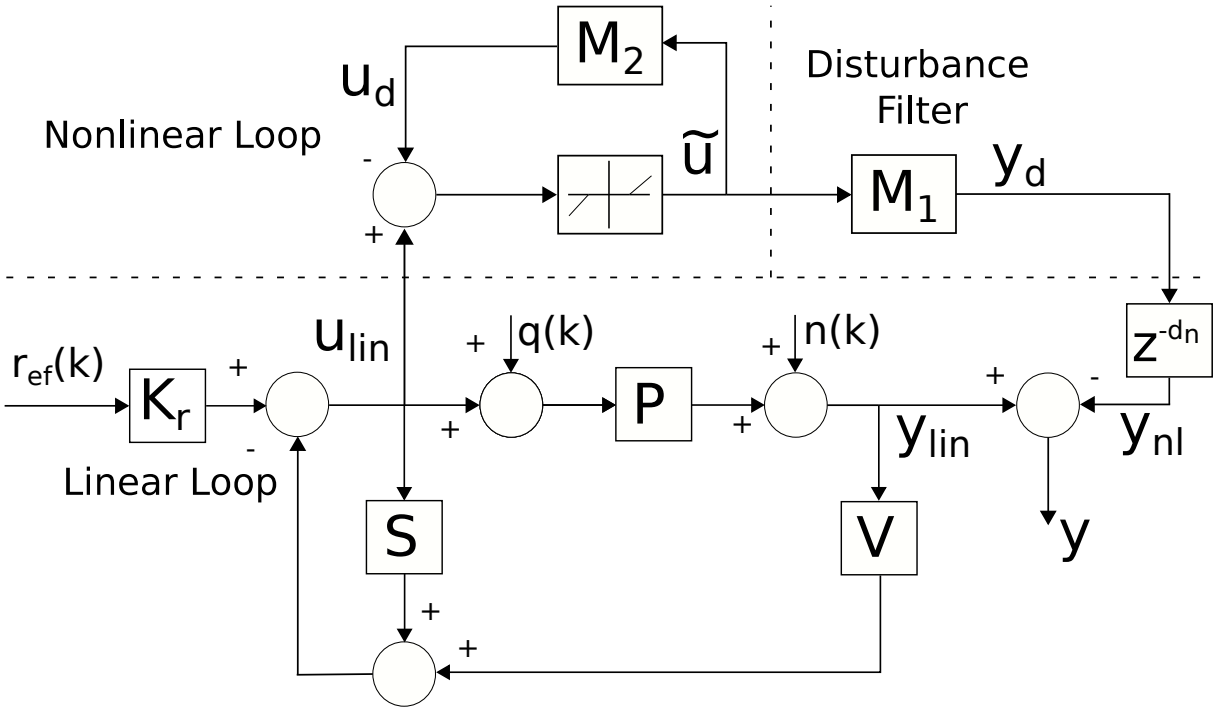

Source: The author.

The linear loop represents how the system would behave in the absence of control saturation. Comparing Eqs. (3.1) and (4.1) it can be seen that all the poles of $M_1(z)$ are within the unit circle, therefore in the nominal case stability of the structure in Fig. 11 depends only upon the stability of the nonlinear loop in Fig. 12.

In addition, performance of the anti-windup system can be measured by choosing an appropriate induced norm for the map from u_{lin} to y_d. From Fig. 12 note that the performance of the anti-windup compensator is related to the size of the map $\tau_{pn} : u_{lin} \to y_d$, which is measured in terms of the $\mathscr{L}_2$ gain (see Definition 2.3.1). The size of this map represents how much the behavior of the system is deviated from the linear nominal system when a saturation event occurs. Assuming that keeping the behavior as close as possible to the linear nominal system is desired, it is said that the anti-windup compensator is successful when the size of this map is small enough.

Finally, the disturbance filter $M_1(z)$ represents how the system recovers after saturation events occurs. Note that when a saturation event ends, the output of the dead-zone nonlinearity $\tilde{u}$ becomes null. However, effects caused by the saturation are not instantaneously over, as the states of the disturbance filter $M_1(z)$ are not null. Therefore, $M_1(z)$ is responsible for determining both speed and manner of recovery of the closed-loop system after saturation ceases.

Consider the state-space realization of the process fast model $G_n(z)$, given by ma-

trices A_p, B_p, C_p, D_p. Without loss of generality, it is assumed that $D_p = 0$, i.e. $G_n(z)$ is strictly proper. In addition, the state-space realization for FIR filters R and F are given by A_R, B_R, C_R, D_R and A_F, B_F, C_F, D_F, respectively. Then, the mapping $\tau_{pn} : u_{lin} \to y_d$ is defined as (see **demonstration** in Appendix A)

$$\tau_{pn} \triangleq \begin{cases} x(k+1) = \bar{A}x(k) + \bar{B}\tilde{u} \\ u_d = \bar{C_2}x(k) + \bar{D_2}\tilde{u} \\ y_d = \bar{C_1}x(k) \\ \tilde{u} = Dz(u_{lin} - u_d) \end{cases} \tag{4.3}$$

where

$$\bar{A} = \begin{bmatrix} A_p - B_p\Delta D_F C_p & -B_p\Delta C_F & -B_p\Delta C_R \\ B_F C_p & A_F & 0 \\ -B_R\Delta D_F C_p & -B_R\Delta C_F & A_R - B_R\Delta C_R \end{bmatrix},$$

$$\bar{B} = \begin{bmatrix} B_p - B_p\Delta D_R \\ 0 \\ B_R - B_R\Delta D_R \end{bmatrix},$$

$$\bar{C_1} = \begin{bmatrix} C_p & 0 & 0 \end{bmatrix}, \quad \bar{C_2} = \begin{bmatrix} -\Delta D_F C_p & -\Delta C_F & -\Delta C_R \end{bmatrix},$$

$$\bar{D_2} = \begin{bmatrix} -\Delta D_R \end{bmatrix}, \quad \Delta = \begin{bmatrix} I - D_R \end{bmatrix}.$$

Using the Lyapunov functional from Theorem 2.2.1 and the $\mathscr{L}_2$ gain from Definition 2.3.1, a necessary but not enough condition for stability is written as

$$\Delta V(x(k)) + y_d^T y_d - \gamma^2 u_{lin}^T u_{lin} < 0. \tag{4.4}$$

Substitution of $x(k+1)$ and y_d as defined in (4.3) leads to

$$x^\intercal(k+1)Px(k+1) - x^\intercal(k)Px(k) + x^\intercal(k)\bar{C_1}^\intercal C_1 x(k) - \gamma^2 u_{lin}^T u_{lin} < 0, \tag{4.5}$$

$$(\bar{A}x(k)+\bar{B}\tilde{u})^{\intercal}P(\bar{A}x(k)+\bar{B}\tilde{u})-x^{\intercal}(k)Px(k)+x^{\intercal}(k)\bar{C_1}^{\intercal}C_1x(k)-\gamma^2u_{lin}^Tu_{lin}<0, \tag{4.6}$$

and by defining $z=\begin{bmatrix}x^T & \tilde{u}^Tu_{lin}^T\end{bmatrix}^T$, inequality (4.6) can be written in an equivalent quadratic form as

$$z^T\begin{bmatrix}\bar{A}^TP\bar{A}-P+\bar{C_1}^T\bar{C_1} & \bar{A}^TP\bar{B} & 0\\ \star & \bar{B}^TP\bar{B} & 0\\ \star & \star & -\gamma^2I\end{bmatrix}z<0. \tag{4.7}$$

Furthermore, from the sector boundedness condition of the deadzone (2.85), the following inequalities hold

$$\begin{aligned}2\tilde{u}^TW\left[u_{lin}-u_d-\tilde{u}\right]\geq 0,\\ 2\tilde{u}^TW\left[u_{lin}-\bar{C}_2x-\bar{D}_2\tilde{u}-\tilde{u}\right]\geq 0,\end{aligned} \tag{4.8}$$

which can be written in matrix form as

$$z^T\begin{bmatrix}0 & -\bar{C_2}^TW & 0\\ \star & -2W(\bar{D}_2+I) & W\\ \star & \star & 0\end{bmatrix}z\geq 0. \tag{4.9}$$

Using the S-procedure inequalities from Equations (4.7) and (4.9) are combined to obtain

$$\begin{bmatrix}\bar{A}^TP\bar{A}-P+\bar{C_1}^T\bar{C_1} & \bar{A}^TP\bar{B}-\bar{C_2}^TW_\tau & 0\\ \star & \bar{B}^TP\bar{B}-2W_\tau(\bar{D}_2+I) & W_\tau\\ \star & \star & -\gamma^2I\end{bmatrix}<0. \tag{4.10}$$

Since τ only appears adjacent to W, the change of variable $V=W_\tau$ is made. In addition, by dividing all terms of (4.10) which do not contain decision variables by γ, the following matrix inequality is obtained (note that division of a matrix variable by a positive

scalar does not alter its positiveness, hence it is not necessary to divide terms which contain P and V by γ),

$$\begin{bmatrix} \bar{A}^T P\bar{A} - P & \bar{A}^T P\bar{B} - \bar{C_2}^T V & 0 \\ \star & \bar{B}^T P\bar{B} - 2V(\bar{D_2} + I) & V \\ \star & \star & -\gamma I \end{bmatrix} - \begin{bmatrix} \bar{C_1}^T \\ 0 \\ 0 \end{bmatrix} \left[-\gamma^{-1}\right] \begin{bmatrix} C_1 & 0 & 0 \end{bmatrix} < 0, \tag{4.11}$$

which is, by Schur complement, equivalent to

$$\begin{bmatrix} \bar{A}^T P\bar{A} - P & \bar{A}^T P\bar{B} - \bar{C_2}^T V & 0 & \bar{C_1}^T \\ \star & \bar{B}^T P\bar{B} - 2V(\bar{D_2} + I) & V & 0 \\ \star & \star & -\gamma I & 0 \\ \star & \star & \star & -\gamma I \end{bmatrix} < 0. \tag{4.12}$$

Note that the procedure above was executed in order to eliminate the quadratic term in decision variable γ. However, there still exists a problem with (4.12); in order to achieve an LMI format (described in Definition 2.1.1), decision variable P cannot stay between matrices $\bar{A}^T$ and $\bar{A}$. Therefore, Schur complement is applied once more to obtain

$$\begin{bmatrix} -P & -\bar{C_2}^T V & 0 & \bar{C_1}^T & \bar{A}^T \\ \star & -V2(\bar{D_2} + I) & V & 0 & \bar{B}^T \\ \star & \star & -\gamma I & 0 & 0 \\ \star & \star & \star & -\gamma I & 0 \\ \star & \star & \star & \star & -P^{-1} \end{bmatrix} < 0. \tag{4.13}$$

Now, it is necessary to eliminate the nonlinear term P^{-1} from (4.13). For this, first $diag(P^{-1}, V^{-1}, I, I, I)$ is used to apply a congruence transformation with (4.13), obtaining

$$\begin{bmatrix} -P^{-1} & -P^{-1}\bar{C_2}^T & 0 & P^{-1}\bar{C_1}^T & P^{-1}\bar{A}^T \\ \star & -2(\bar{D_2} + I)V^{-1} & I & 0 & V^{-1}\bar{B}^T \\ \star & \star & -\gamma I & 0 & 0 \\ \star & \star & \star & -\gamma I & 0 \\ \star & \star & \star & \star & -P^{-1} \end{bmatrix} < 0. \tag{4.14}$$

Then, by defining new variables $Q = P^{-1}$ and $U = V^{-1}$, the following LMI is obtained

$$\Upsilon_{nom} = \begin{bmatrix} -Q & -Q\bar{C_2}^T & 0 & Q\bar{C_1}^T & Q\bar{A}^T \\ \star & -2(\bar{D_2}+I)U & I & 0 & U\bar{B}^T \\ \star & \star & -\gamma I & 0 & 0 \\ \star & \star & \star & -\gamma I & 0 \\ \star & \star & \star & \star & -Q \end{bmatrix} < 0, \tag{4.15}$$

with $Q > 0$, $U > 0$ and $\gamma > 0$. Next, the following theorem establishes a condition to prove stability of the AWSDTC in the nominal case.

Theorem 4.1.1 *The closed-loop system in Figure 11 is internally stable for the nominal case ($P_n(z) = P(z)$) if there exist symmetric matrices $Q > 0, U > 0$, and scalar $\gamma > 0$ such that $\Upsilon_{nom} < 0$ is feasible. Moreover, the $\mathscr{L}_2$ gain is computed by minimizing γ subject to the above constraints.*

4.2 Robust Stability Analysis

In this Section, stability results are presented for the closed-loop system in the presence of model uncertainties. The analysis is carried out in such a way that six theorems are obtained for six different scenarios in the presence of model uncertainties. For all the situations, though, the process delay is considered to be unknown, bounded, and possibly time-varying.

Initially, in Subsection 4.2.1, an equivalent representation of the SDTC with actuator saturation in the presence of norm-bounded uncertainties is obtained. This is the most general case, hence it is useful to obtain the equivalent representation in such a way, as it will become clearer latter. Then, the rest of this Section is organized as follows.

- Subsection 4.2.2 presents three robust stability results in the LMI format for the SDTC (without saturation nonlinearity): (i) stability for uncertain time-varying delay without uncertainties in the process fast-model, (ii) stability in the presence of uncertain time-varying delay processes plus polytopic uncertainties in the process fast-model, (iii) stability in the presence of uncertain time-varying delay processes plus norm-bounded uncertainties in the process fast-model
- In Subsection 4.2.3, other three cases with the same uncertainties of Subsection 4.2.2 are presented; however, actuator saturation is considered (AWSDTC), thus

achieving the ultimate goal of this work.

4.2.1 Equivalent State-Space Delay Representation

Consider the anti-windup SDTC implementation structure in Figure 10; moreover, consider that the process delay is bounded and time-varying such as $h_0 \leq \tau_k \leq h_1$, and norm-bounded uncertainties in the delay free plant model $G_n(z)$. For the purposes of internal stability analysis, external signals can be considered null $(r_{ef}(k) = 0, q(k) = 0, n(k) = 0)$. By defining $Dz(u(k)) = \tilde{u}(k)$ and using identity (2.82) one obtains

$$u_a(k) = sat(u(k)) = u(k) - \tilde{u}(k).$$

Then, the state-space representation of the discrete process $P(z)$, the subsystem $S(z)$ (3.15), and the robustness filter $V(z)$ are defined by the following equations

$$P(z) = \begin{cases} x_p(k+1) = \hat{A_p} x_p(k) + \hat{B_p} u_a(k - \tau_k) \\ y(k) = C_p x_p(k) \end{cases}$$

$$S(z) = \begin{cases} x_s(k+1) = A_s x_s(k) + B_s u_a(k) \\ y_s(k) = C_s x_s(k) \end{cases}$$

$$V(z) = \begin{cases} x_v(k+1) = A_v x_v(k) + B_v y(k) \\ y_v(k) = C_v x_v(k) + D_v y(k) \end{cases}$$

where $\hat{A_p} = A_p + \Delta A_p$, $\hat{B_p} = B_p + \Delta B_p$, and the uncertainties are of the form $\begin{bmatrix} \Delta A_p & \Delta B_p \end{bmatrix} = E\delta(k) \begin{bmatrix} H_A & H_B \end{bmatrix}$. The matrices E, H_A and H_B are constant and known, whereas $\delta(k)$ is an unknown time-varying matrix satisfying

$$\delta^T(k)\delta(k) \leq I. \tag{4.16}$$

After some algebraic manipulations the equivalent state space closed-loop representation is obtained as

$$\begin{cases} x(k+1) = [A+\Delta A(k)]x(k) + [A_d+\Delta A_d(k)]x(k-\tau_k) \\ \qquad\qquad +B\tilde{u}(k) + [B_d+\Delta B_d(k)]\tilde{u}(k-\tau_k) \\ \tilde{u}(k) = Dz(Cx(k)) \end{cases} \tag{4.17}$$

where the process delay t_k appears in the states of the system and

$$x(k) = \begin{bmatrix} x_p(k)^T & x_s(k)^T & x_v(k)^T \end{bmatrix}^T \tag{4.18}$$

$$A = \begin{bmatrix} A_p & 0 & 0 \\ -B_s D_v C_p & A_s - B_s C_s & -B_s C_v \\ B_v C_p & 0 & A_v \end{bmatrix} \tag{4.19}$$

$$\begin{gathered} \Delta A(k) = \overline{E}\,\delta(k)\overline{H_A} \\ \overline{E} = \begin{bmatrix} E & 0 & 0 \end{bmatrix}^T, \quad \overline{H_A} = \begin{bmatrix} H_A & 0 & 0 \end{bmatrix} \end{gathered} \tag{4.20}$$

$$A_d = \begin{bmatrix} -B_p D_v C_p & -B_p C_s & -B_p C_v \\ 0 & 0 & 0 \\ 0 & 0 & 0 \end{bmatrix} \tag{4.21}$$

$$\begin{gathered} \Delta A_d(k) = \overline{E}\,\delta(k)\overline{H_{Ad}} \\ \overline{H_{Ad}} = \begin{bmatrix} -H_B D_v C_p & -H_B C_s & -H_B C_v \end{bmatrix} \end{gathered} \tag{4.22}$$

$$B = \begin{bmatrix} 0 \\ -B_s \\ 0 \end{bmatrix}, B_d = \begin{bmatrix} -B_p \\ 0 \\ 0 \end{bmatrix} \tag{4.23}$$

$$\Delta B_d(k) = \overline{E}\,\delta(k)\overline{H_B}, \quad \overline{H_B} = -H_B \tag{4.24}$$

$$C = \begin{bmatrix} -D_v C_p & -C_s & -C_v \end{bmatrix} \tag{4.25}$$

4.2.2 Robust stability of the SDTC with time-varying delay

4.2.2.1 Case 1 - SDTC with time-varying process delay

Consider the equivalent state space representation of the AW SDTC in (4.17) without actuator saturation. In this situation, $sat(u(k))$ is always equal to $u(k)$, thus $u\tilde{(k)} = Dz(u(k)) = 0$ for all $k > 0$ and the AWSDTC reduces simply to the original SDTC. Furthermore, when there are no uncertainties in the process fast-model ($\Delta A = 0$ and $\Delta A_d = 0$), closed-loop system (4.17) reduces to

$$x(k+1) = Ax(k) + A_d x(k-\tau_k),\ k \in \mathbb{Z}^+,\ \tau_k \in \mathbb{N},\ h_0 \leq \tau_k \leq h_1, \tag{4.26}$$

which is equal to the system (2.47) that has been previously studied in Chapter 2. Therefore, the Corollary below easily follows from Theorem 2.2.2 to establish stability of the SDTC in this scenario.

Corollary 4.2.1 *The SDTC is asymptotically stable for all time-varying delays $h_0 \leq \tau_k \leq h_1$ if there exists matrices $P > 0, R > 0, S > 0, R_1 > 0, S_1 > 0, P_2, P_3, S_{12}$ such that LMIs* (2.64) *and* (2.59) *are feasible, where closed-loop matrices A and A_d are defined by Equations* (4.19) *and* (4.21)*, respectively.*

4.2.2.2 Case 2 - SDTC with time-varying process delay and polytopic uncertainties

Once more, the fundamentals for this case have already been demonstrated in Chapter 2. Consider that state-space matrices A_p and B_p contain structured model uncertainties as polytopic uncertainties. Since closed-loop matrices A and A_d depend on A_p and B_p, the aforementioned uncertainties can be mapped to A and A_d as follows

$$\Gamma = \begin{bmatrix} A & A_d \end{bmatrix}, \quad \Gamma \in \Pi\{\Gamma_j, j = 1, ..., M\} \tag{4.27}$$

$$\Gamma = \sum_{j=1}^{M} \omega_j \Gamma_j, \quad \text{for some } 0 \leq \omega_j \leq 1, \sum_{j=1}^{M} \omega_j = 1, \tag{4.28}$$

where $\Gamma_j = \begin{bmatrix} A^j & A_d^j \end{bmatrix}$ describes the M vertices of the polytope. Thus, the problem of guaranteeing closed-loop stability of the SDTC in this scenario is equivalent to the problem in Corollary 2.2.1. Then, the Corollary below clearly holds

Corollary 4.2.2 *Assume that* (2.59) *and M LMIs* (2.64) *written in the vertices of* Γ_j *as described by Equations* (4.27) *and* (4.28) *are feasible for the same matrices* $P > 0, R > 0, S > 0, R_1 > 0, S_1 > 0, P_2, P_3$ *and* S_{12}. *Then,*

$$\sum_{j=1}^{M} \omega_j \Upsilon_{11}^j = \Upsilon_{11} < 0, \tag{4.29}$$

and the SDTC closed-loop system with polytopic type uncertainties described by (4.27) *and* (4.28) *is asymptotically stable for all time-varying delays* $h_0 \leq \tau_k \leq h_1$.

4.2.2.3 Case 3 - SDTC with time-varying process delay and norm-bounded uncertainties

For the case of norm-bounded uncertainties, the SDTC equivalent closed-loop is written (similarly to (2.71)) as

$$x(k+1) = [A + \Delta A(k)]x(k) + [A_d + \Delta A_d(k)]x(k - \tau_k), \tag{4.30}$$

where matrices A, $\Delta A = \overline{E}\delta(k)\overline{H_A}$, A_d and $\Delta A_d = \overline{E}\delta(k)\overline{H_{Ad}}$ have been defined in (4.19), (4.20), (4.21) and (4.22), respectively. Then, from Corollary (2.2.2) it follows that

Corollary 4.2.3 *The SDTC is asymptotically stable for all time-varying delays* $h_0 \leq \tau_k \leq h_1$ *and all* $\delta(k)$ *satisfying Equation* (4.16) *if there exists matrices* $P > 0, R > 0, S > 0, R_1 > 0, S_1 > 0, P_2, P_3, S_{12}$ *and scalar* $\varepsilon > 0$ *such that LMIs* (2.76) *and* (2.59) *are feasible.*

4.2.3 Robust stability of the AWSDTC with time-varying delay

4.2.3.1 Case 4 - AWSDTC with time-varying process delay

In the AWSDTC case ($Dz(u) = \tilde{u} \neq 0$) without uncertainties in the process fast-model ($\Delta A = 0$ and $\Delta A_d = 0$), closed-loop system (4.17) reduces to

$$\begin{cases} x(k+1) = Ax(k) + A_d x(k - \tau_k) + B\tilde{u}(k) + B_d\tilde{u}(k - \tau_k), \\ \tilde{u}(k) = Dz(Cx(k)), \end{cases} \tag{4.31}$$

thus, the definition of $x(k+1)$ is different from (4.26), and therefore it is necessary to obtain a new equation by applying the descriptor method to (4.31)

$$DESC_{sat}(k) \equiv 2[x^{\intercal}(k)P_2^{\intercal} + \bar{y}^{\intercal}(k)P_3^{\intercal}][(A-I)x(k) + A_d x(k-\tau_k) + B\tilde{u}(k) + B_d\tilde{u}(k-\tau_k) - \bar{y}] = 0. \tag{4.32}$$

Furthermore, the sector boundedness condition of the deadzone (2.85) is applied to (4.17), obtaining

$$2\tilde{u}^T W\left[Cx(k) - \tilde{u}(k)\right] \geq 0, \quad \text{for some } W > 0. \tag{4.33}$$

$$2\tilde{u}^T(k-\tau_k)W\left[Cx(k-\tau_k) - \tilde{u}(k-\tau_k)\right] \geq 0, \quad \text{for some } W > 0. \tag{4.34}$$

Then, by addition of (4.32) and (4.34) to Lyapunov condition (2.60) and definition of

$$\eta_{case_4}(k) = col\{x(k), \bar{y}(k), x(k-h_0), x(k-h_1), x(k-\tau_k), \tilde{u}(k), \tilde{u}(k-\tau_k)\}, \tag{4.35}$$

it is obtained that

$$V(x(k-1)) - V(x(k)) \leq \eta_{case_4}(k)^T \Phi_{11} \eta_{case_4}(k) \leq -\alpha|x(k)|^2, \tag{4.36}$$

is satisfied for some $\alpha > 0$, where Φ_{11} is defined in the following Corollary which establishes stability of the AWSDTC in the this case.

Corollary 4.2.4 *The AWSDTC is asymptotically stable for all time-varying delays $h_0 \leq \tau_k \leq h_1$ if there exists matrices $P > 0, R > 0, S > 0, R_1 > 0, S_1 > 0, W > 0, P_2, P_3, S_{12}$ such that LMIs*

(2.59) *and*

$$\Phi_{11} = \begin{bmatrix} \Psi_{11} & \Psi_{12} & R & 0 & P_2^T A_d & P_2^T B + C^T W & P_2^T B_d \\ \star & \Psi_{22} & 0 & 0 & P_3^T A_d & P_3^T B & P_3^T B_d \\ \star & \star & \Psi_{33} & S_{12} & R - S_{12} & 0 & 0 \\ \star & \star & \star & \Psi_{44} & R_1 - S_{12}^T & 0 & 0 \\ \star & \star & \star & \star & \Psi_{55} & 0 & C^T W^T \\ \star & \star & \star & \star & \star & -2W & 0 \\ \star & \star & \star & \star & \star & \star & -2W \end{bmatrix} \leq 0 \tag{4.37}$$

are feasible.

4.2.3.2 Case 5 - AWSDTC with time-varying process delay and polytopic uncertainties

Once again, consider polytopic uncertainties in state-space matrices A_p and B_p. Since closed-loop matrices A, A_d and B_d depend on A_p and B_p, those uncertainties can be mapped to A, A_d and B_d, and the following polytope can be defined

$$\Gamma^{sat} = \begin{bmatrix} A & A_d & B_d \end{bmatrix}, \quad \Gamma^{sat} \in \Pi\{\Gamma_j^{sat}, j = 1, ..., M\}, \tag{4.38}$$

$$\Gamma^{sat} = \sum_{j=1}^{M} \omega_j \Gamma_j^{sat}, \quad \text{for some } 0 \leq \omega_j \leq 1, \sum_{j=1}^{M} \omega_j = 1, \tag{4.39}$$

where $\Gamma_j^{sat} = \begin{bmatrix} A^j & A_d^j & B_d^j \end{bmatrix}$ describes the M vertices of the polytope. Then, the Corollary below can be stated

Corollary 4.2.5 *Assume that* (2.59) *and M LMIs* (4.37) *written in the vertices of* Γ_j^{sat}

$$\Phi_{11}^j = \begin{bmatrix} \Psi_{11}^j & \Psi_{12}^j & R & 0 & P_2^T A_d^j & P_2^T B + C^T W & P_2^T B_d^j \\ \star & \Psi_{22} & 0 & 0 & P_3^T A_d^j & P_3^T B & P_3^T B_d^j \\ \star & \star & \Psi_{33} & S_{12} & R - S_{12} & 0 & 0 \\ \star & \star & \star & \Psi_{44} & R_1 - S_{12}^T & 0 & 0 \\ \star & \star & \star & \star & \Psi_{55} & 0 & C^T W^T \\ \star & \star & \star & \star & \star & -2W & 0 \\ \star & \star & \star & \star & \star & \star & -2W \end{bmatrix} \leq 0 \tag{4.40}$$

are feasible for the same matrices $P > 0, R > 0, S > 0, R_1 > 0, S_1 > 0, W > 0, P_2, P_3$ *and* S_{12}. *Then,*

$$\sum_{j=1}^{M} \omega_j \Phi_{11}^j = \Phi_{11} < 0, \tag{4.41}$$

and the AWSDTC closed-loop system with polytopic type uncertainties described by (4.38) *and* (4.39) *is asymptotically stable for all time-varying delays* $h_0 \leq \tau_k \leq h_1$.

4.2.3.3 Case 6 - AWSDTC with time-varying process delay and norm-bounded uncertainties

In this case, norm-bounded uncertainties are considered in the process. Thus, matrices ΔA, ΔA_d and ΔB_d exist in the closed-loop, as described by (4.17). LMI (4.37) is affine in the system matrices, thus A, A_d and B_d are replaced in Φ_{11} by $A + \overline{E}\delta(k)\overline{H_A}$, $A_d + \overline{E}\delta(k)\overline{H_{Ad}}$ and $B_d + \overline{E}\delta(k)\overline{H_B}$, respectively. Then, separation of terms with uncertainties leads to the following inequality

$$\Phi_{11} + \Phi_{12}\delta(k)\Phi_{13}^T + \Phi_{13}\delta(k)^T\Phi_{12}^T < 0. \tag{4.42}$$

where

$$\Phi_{12} = \begin{bmatrix} P_2^T\overline{E} \\ P_3^T\overline{E} \\ 0 \\ 0 \\ 0 \\ 0 \\ 0 \end{bmatrix}, \quad \Phi_{13} = \begin{bmatrix} \overline{H_A}^T \\ 0 \\ 0 \\ 0 \\ \overline{H_{Ad}}^T \\ 0 \\ \overline{H_B}^T \end{bmatrix}. \tag{4.43}$$

Then, by the application of the following inequality for some scalar $\varepsilon > 0$ (XIE, 1996)

$$\Phi_{12}\delta(k)\Phi_{13}^T + \Phi_{13}\delta(k)^T\Phi_{12}^T \leq \varepsilon^{-1}\Phi_{12}\Phi_{12}^T + \varepsilon\Phi_{13}\Phi_{13}^T, \tag{4.44}$$

and Schur complements, the following LMI is obtained

$$\begin{bmatrix} \Phi_{11} & \Phi_{12} & \varepsilon\Phi_{13} \\ \star & -\varepsilon & 0 \\ \star & \star & -\varepsilon \end{bmatrix} < 0. \tag{4.45}$$

Finally, the following Corollary establishes robust stability of the AWSDTC with norm-bounded uncertainties and time-varying process delay.

Corollary 4.2.6 *The AWSDTC is asymptotically stable for all time-varying delays* $h \leq \tau_k \leq h_1$ *and all* $\delta(k)$ *satisfying Equation* (4.16) *if there exists matrices* $P > 0, R > 0, S > 0, R_1 > 0, S_1 > 0, W > 0, P_2, P_3, S_{12}$ *and scalar* $\varepsilon > 0$ *such that LMIs* (4.45) *and* (2.59) *are feasible.*

5 RESULTS

This Chapter has the following specific objectives: (i) to use simulation results to establish a fair comparison between the proposed anti-windup SDTC and other anti-windup controllers, (ii) to use a simulation example to compare the AWSDTC with the regular SDTC, (iii) to use a first-order process to show how different choices in tuning parameters and modeling uncertainties can affect the delay interval for which stability is guaranteed, (iv) to use a practical experiment to proof real life applicability of the AWSDTC. Section 5.1 is aimed at achieving the first three goals, whereas Section 5.2 is shortly presented to fulfill the last.

5.1 Simulation Results

This section first presents a simulation case study using the integrative process presented (ZHANG; JIANG, 2008). This example is used to establish a fair comparison with other anti-windup strategies. Therefore, the delay was initially considered to be bounded and uncertain but time-invariant, as in the aforementioned work. In the second example, the same first-order process from (ZHANG; JIANG, 2008) is used to analyse robust closed-loop stability of the AWSDTC in the presence of uncertain time-varying delays and its relation with the user tuning parameter β (3.10). Later, a second-order process is used to compare the AWSDTC with the SDTC and show the relation between the tuning of the primary controller and the anti-windup performance by means of the $\mathscr{L}_2$ gain. The considered controllers were evaluated under input disturbances and step reference variations.

5.1.1 Example 1 - Comparison with other anti-windup controllers

This example presents comparative simulation results obtained with the following four controllers: an input constrained MPC (CAMACHO; BORDONS, 2004), the controller reported in (ZHANG; JIANG, 2008), and the proposed anti-windup SDTC. For this purpose, the following process model presented in (ZHANG; JIANG, 2008) is considered:

$$P(s) = \frac{e^{-5s}}{s}.$$

By using a sampling time $T = 0.2$ the following discretized system is obtained:

$$P(z) = \frac{0.2}{z-1} z^{-25}.$$

The input limits are $u_l = -1$ and $u_u = 1$. The parameters of the (ZHANG; JIANG, 2008) controller are defined in the paper. The MPC uses the following model to compute the predictions:

$$(1-q^{-1})y(t) = 0.1u(t-1-d_n) + \frac{(1-\beta_{mpc}q^{-1})^2}{(1-q^{-1})}e_n(t), \tag{5.1}$$

where q^{-1} is the backward shift operator, $\beta_{mpc} = e^{-T/2.4}$, $d_n = 0.5/T = 25$, and $e_n(t)$ is a white noise. The MPC tuning parameters are: the limits of the prediction windows $N_1 = d+1$, $N_2 = d+100$, the control horizon $N_u = 70$, and the control weights defined as $\lambda_1 = 0$ and $\lambda_i = 250$, $i = 2,\ldots,N_u$. The MPC was tuned in order to present a step response quite similar to (ZHANG; JIANG, 2008) controller in the nominal case without input saturation.

For the AWSDTC controller three different tunings are considered. The first one, named AWSDTC$_1$, aims a step response close to the one observed for the MPC. Thus, the AWSDTC$_1$ controller is given by:

$$K_r = 0.4,\ f_0 = 0.4, \text{ and } V(z^{-1}) = \frac{0.1574 - 0.1549z^{-1}}{(1-0.92z^{-1})^2}.$$

On the other hand, the second one (AWSDTC$_2$) was tuned aiming an improved disturbance rejection under input saturation, leading to the following parameters:

$$K_r = 0.2,\ f_0 = 0.2,\ \text{ and } V(z^{-1}) = \frac{0.2326 - 0.2289z^{-1}}{(1-0.865z^{-1})^2}.$$

Figures 13 and 14 show the simulation results for a step reference for the AWSDTC$_1$ and AWSDTC$_2$. An input disturbance pulse with amplitude of -1.5 was applied from $t = 40$ s to $t = 50$ s. A step input disturbance with amplitude of -0.5 was applied at $t = 100$ s.

Fig. 13 shows the simulation results without uncertainties. As it can be observed all the anti-windup controllers follow the reference in a similar way.

On the other hand, in the case of both input pulse disturbance and input saturation, the proposed AWSDTC$_2$ controller is the only one which does not present undesired overshoots. For the step input disturbance the control action is not saturated and the performance of all controllers are nearly the same. It is worth to mention that the predictor of the anti-windup SDTC can be interpreted as an observer. According to (3.10), β is the only free tuning parameter of the robustness filter, and can be used to speed up disturbance rejection or improve robustness. However when one is prioritized the other is impaired. It can be observed that the β parameter

Figure 13 – Simulation results for Example 1 (no uncertainties), Z&J is Zhang and Jiang (2008).

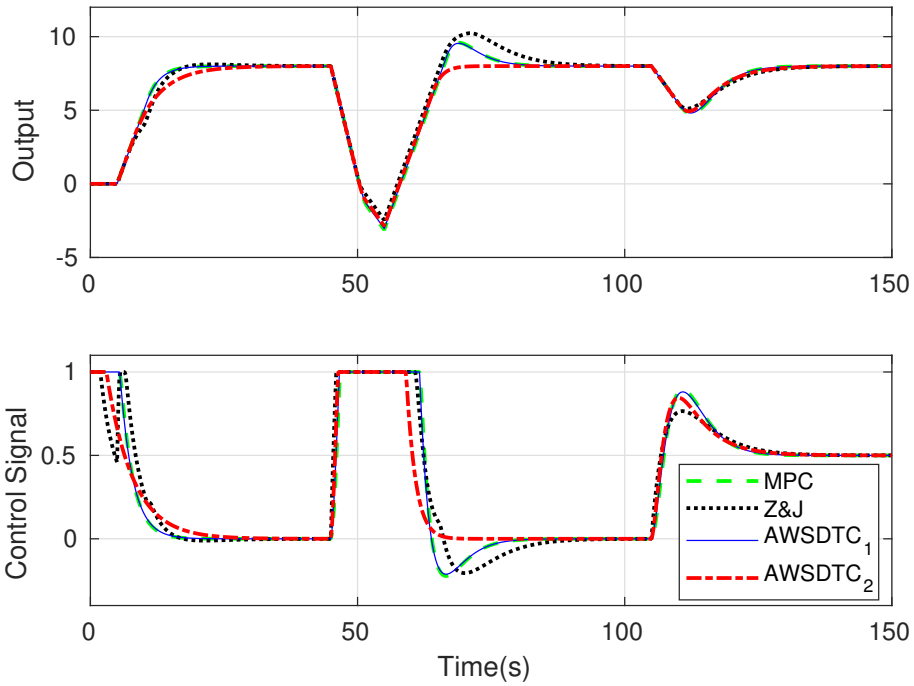

Source: The author.

Figure 14 – Simulation results for Example 1 (20% dead-time uncertainty), Z&J is (ZHANG; JIANG, 2008).

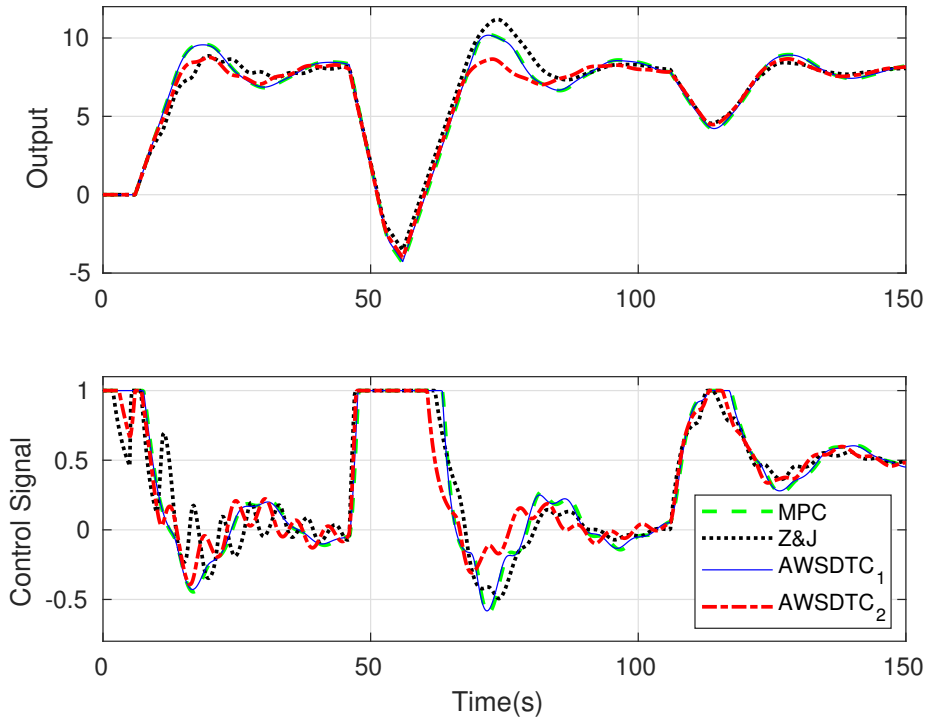

Source: The author.

of $V(z)$ for the proposed SDTC$_2$ is smaller than the SDTC$_1$, which means lower robustness and better speed performance, as can be seen in Fig. 13.

Fig. 14 shows simulation results using $+20\%$ dead-time uncertainty. It can be seen that the proposed AWSDTC$_2$ still presents the best response in this situation. It is important to highlight that the proposed anti-windup SDTC achieves similar or better performance than a MPC, which is a more complex controller.

In order to establish a fair comparison with a recently published anti-windup strategy (FLESCH *et al.*, 2017), the AWSDTC$_3$ was tuned to yield a similar set-point tracking response by using the following parameters

$$K_r = 0.5,\ f_0 = 0.5,\ \text{ and } V(z^{-1}) = \frac{2.17 - 1.925z^{-1}}{(1-0.3z^{-1})^2}.$$

Figure 15 shows the results for the nominal case, while Figure 16 presents the results using $+5\%$ dead-time uncertainty. Notice that in the nominal case the AWSDTC$_3$ does not present overshoots, while the controller from Flesch *et al.* (2017) presents peaks after both the pulse and step disturbances. Also note (from Figure 16) that even a uncertainty as small as $+5\%$ in the dead-time can seriously harm the performance of the compared controller.

Figure 15 – Simulation results for Example 1 (no uncertainties).

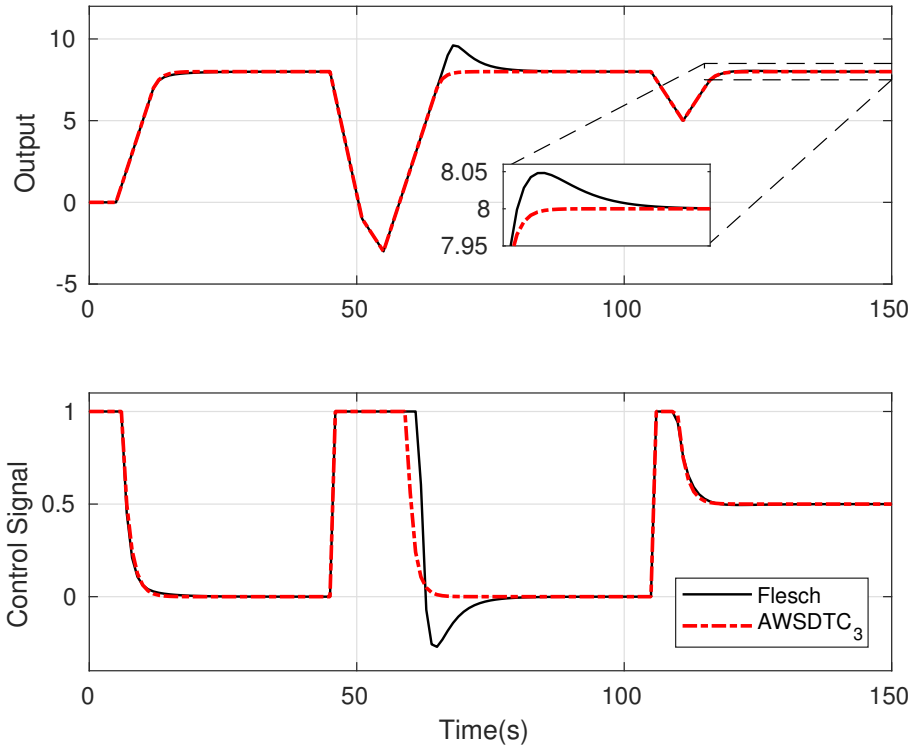

Source: The author.

Figure 16 – Simulation results for Example 1 (5% dead-time uncertainty).

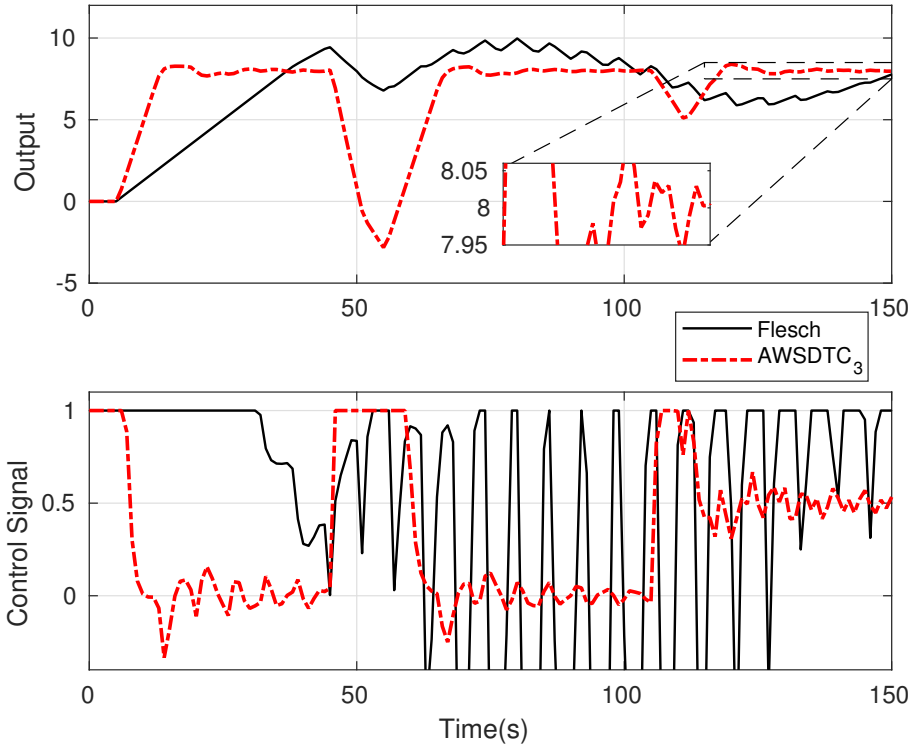

Source: The author.

5.1.2 Example 2 - Robust stability analysis

The nominal state-space realization of the FOPDT process studies in Example 1 when a sampling time $T = 0.5s$ is used is given by $A_p = 1$, $B_p = 1$, $C_p = 0.5$ and $d_n = 10$. Consider the following controller tuning for this example (AWSDTC$_1$):

$$K_r = 0.08,\ f_0 = 0.08,\ \text{ and } V(z^{-1}) = \frac{0.03021 - 0.0297z^{-1}}{(1-0.92z^{-1})^2}.$$

Initially, consider that there are no uncertainties in the plant fast-model and no actuator saturation. Then, by means of the LMIs in Corollary 4.2.1 (Case 1) it is possible to guarantee stability of the closed-loop for all time-varying delay such as $d_n - 10 \leq \tau_k \leq d_n + 11$ ($h_0 = 0$ and $h_1 = 21$).

Consider now that norm-bounded uncertainties exist with $H_A = -0.01$, $H_B = 0.1$ and $E = 0.1$ such that the state-state realization of the real process is given by $\hat{A_p} = A_p + \Delta A_p$, $\hat{B_p} = B_p + \Delta B_p$, where $\begin{bmatrix}\Delta A_p & \Delta B_p\end{bmatrix} = E\delta(k)\begin{bmatrix}H_A & H_B\end{bmatrix}$ and $\delta(k)$ satisfies Equation (4.16). Then, by means of the LMIs in Corollary 4.2.3 (Case 3) it is possible to guarantee stability of the closed-loop for all time-varying delay such as $d_n - 10 \leq \tau_k \leq d_n + 10$ ($h_0 = 0$ and $h_1 = 20$).

For the cases with actuator saturations, both Corollaries 4.2.4 (Case 4) and 4.2.6 (Case 6) guarantee stability of the closed-loop for all time-varying delay such as $d_n - 4 \leq \tau_k \leq d_n + 4$ ($h_0 = 6$ and $h_1 = 16$).

Consider now that the value of β in this example is reduced from 0.92 to 0.865, thus the new controller (AWSDTC$_2$) has the following parameters:

$$K_r = 0.08,\ f_0 = 0.08,\ \text{ and } V(z^{-1}) = \frac{0.07117 - 0.06971z^{-1}}{(1 - 0.865z^{-1})^2}.$$

In this scenario, both Corollaries 4.2.1 (Case 1) and 4.2.3 (Case 3) guarantee stability of the closed-loop for all time-varying delay such as $d_n - 9 \leq \tau_k \leq d_n + 9$ ($h_0 = 1$, $h_1 = 19$). Furthermore, both Corollaries 4.2.4 (Case 4) and 4.2.4 (Case 6) guarantee stability of the closed-loop for all time-varying delay such as $d_n - 2 \leq \tau_k \leq d_n + 2$ ($h_0 = 8$, $h_1 = 12$). Thus, all the stability intervals were reduced when β was reduced, making it evident that as the regular SDTC the proposed anti-windup SDTC is still sensitive to this tuning parameter (see Table 1). Therefore, it is necessary to take precautions when choosing the appropriate value of β; higher values yield more robustness to the closed-loop in exchange to becoming more susceptible to windup effects due to slow modes in Equation (3.17), as evidenced in the simulation results of Example 1 where the *AWSDTC* with lower β presented better time-responses.

To conclude this Subsection, Figure 17 shows the time-response of the (AWSDTC$_1$) in the presence of a time-varying delay $d_n - 4 \leq \tau_k \leq d_n + 4$ and cited norm-bounded uncertainties. The control bound for this example was set in $\bar{u} = 0.05$. A step-like input disturbance of +0.01 was applied to the control signal at time $t = 100s$ and measurement noise was applied in the last $20s$ of simulation. The (AWSDTC$_1$) is capable of rejecting the disturbance and follow the reference, demonstrating effectiveness of the anti-windup strategy even in the presence of time-varying delays and norm-bounded uncertainties. In addition, Figure 18 shows the profile of the time-varying delay.

Table 1 – Delay time-varying intervals for stability

Controller	Case 1	Case 3	Case 4	Case 6
AWSDTC$_1$	($h_0 = 0$ and $h_1 = 21$)	($h_0 = 0$ and $h_1 = 20$)	($h_0 = 6$ and $h_1 = 16$)	($h_0 = 6$ and $h_1 = 16$)
AWSDTC$_2$	($h_0 = 1$ and $h_1 = 19$)	($h_0 = 1$ and $h_1 = 19$)	($h_0 = 8$ and $h_1 = 12$)	($h_0 = 8$ and $h_1 = 12$)

Source: The author.

Figure 17 – Simulation results for Example 2

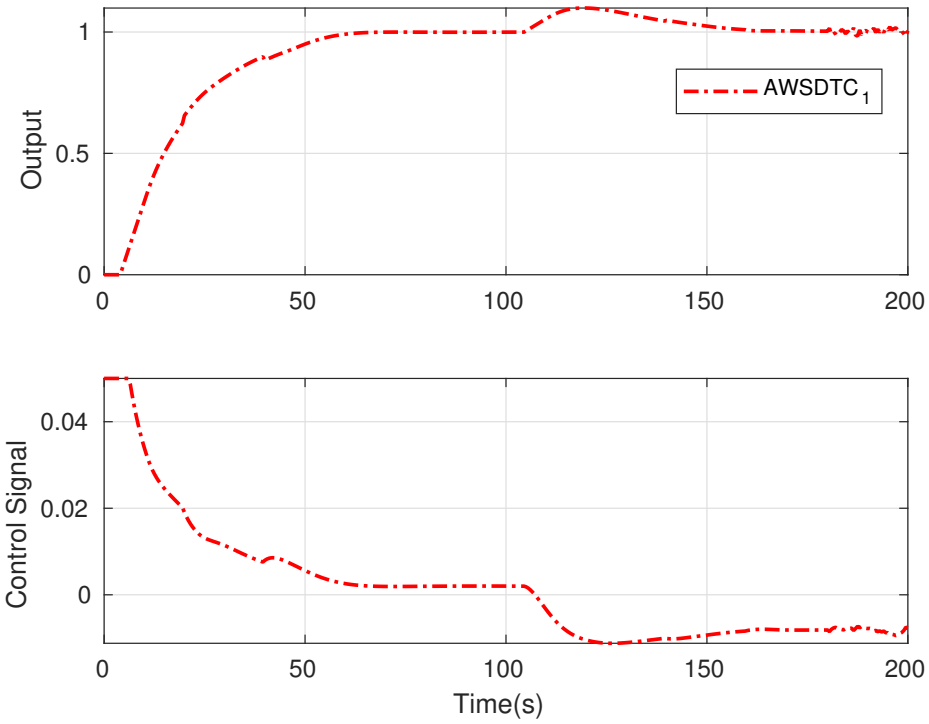

Source: The author.

Figure 18 – Time varying delay for Example 2.

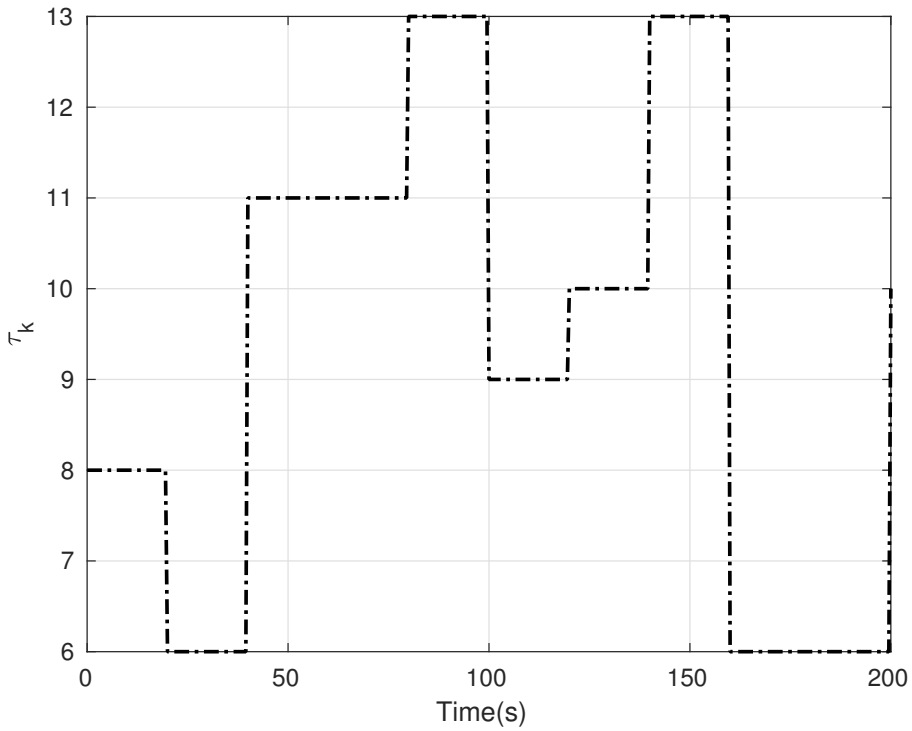

Source: The author.

5.1.3 Example 3 - Comparison with regular SDTC and $\mathscr{L}_2$ gain analysis

In order to validate the proposed anti-windup strategy (AWSDTC) against the traditional SDTC, which does not include the saturation model to the control structure, consider the problem of controlling the following stable Second Order Plus Dead-time (SOPDT) system

$$P(s) = \frac{e^{-0.5s}}{(s+1)(s+2)}.$$

By using a sampling time $T = 0.2$ the following discretized system is obtained:

$$P(z) = \frac{0.01643z^{-1} + 0.01345z^{-2}}{1 - 1.489z^{-1} + 0.5488z^{-2}} z^{-3}.$$

The primary controller was tuned to obtain set-tracking poles (3.1) equal to 0.5, 0.7, and 0.9, and robustness filter was tuned with $\beta = 0.865$ for both the AWSDTC and the SDTC controllers, thus obtaining

$$K_r = 0.502,\ R = -0.593z^{-1},\ F = -1.09 + 0.7782z^{-1}, \text{ and}$$
$$V(z^{-1}) = \frac{0.01553 - 0.02147z^{-1} + 0.007184z^{-2}}{(1 - 0.865z^{-1})^3}.$$

Figure 19 shows the results for a simulation with the same disturbances previously used in Example 1. As expected, the AWSDTC presented better response due to the windup effects that slowed down the pulse disturbance rejection of the SDTC without the saturation model.

In order to validate the nominal stability analysis of the AWSDTC, which uses a decoupled structure between the nonlinear and linear responses, a simulation was executed and shown in Figure (20). Note that the influence of the nonlinear loop and disturbance filter y_{nl} (refer to Figure 12) is mainly present during the rejection of the pulse disturbance. This happens because the AWSDTC control signal remains saturated for some time during this event. Also note that $y = y_{lin} - y_{nl}$ is equal to the AWSDTC output response shown in Figure 19, as it should. By using Theorem 4.1.1, the $\mathscr{L}_2$ gain of the AWSDTC for this situation was calculated as $\gamma = 0.68651$.

From Figure 12 it became clear that the $\mathscr{L}_2$ gain of the AWSDTC in the nominal case depends only upon the process fast-model G_n, and FIR filters R, F, which are used to set the poles of the reference-tracking response (3.1). Thus, Figure 21 was plotted (by using Theorem

Figure 19 – Simulation results for Example 3.

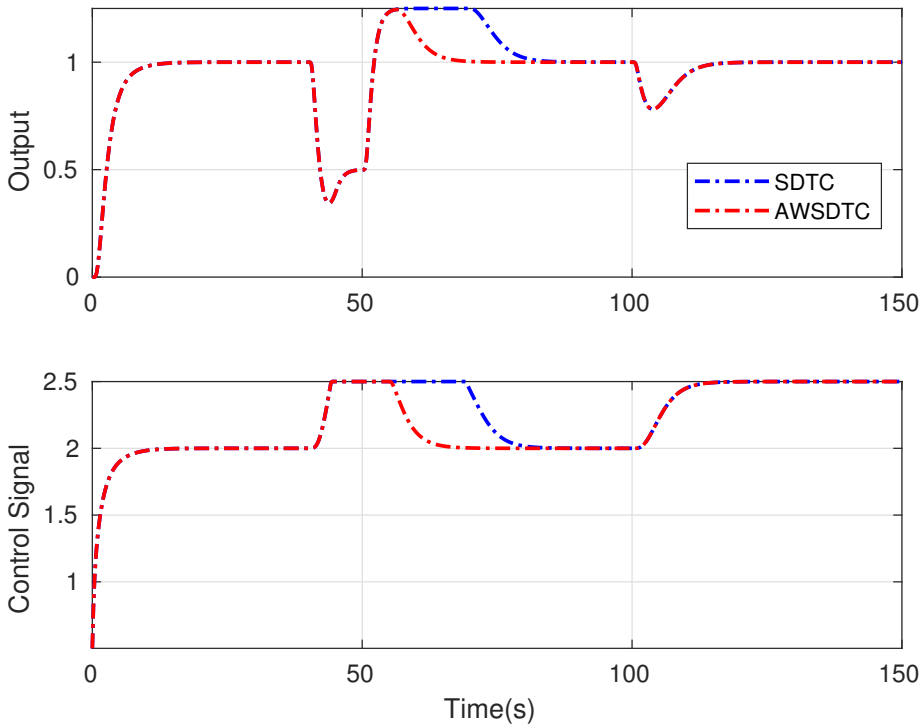

Source: The author.

Figure 20 – Nonlinear and linear components of the AWSDTC output - Example 3.

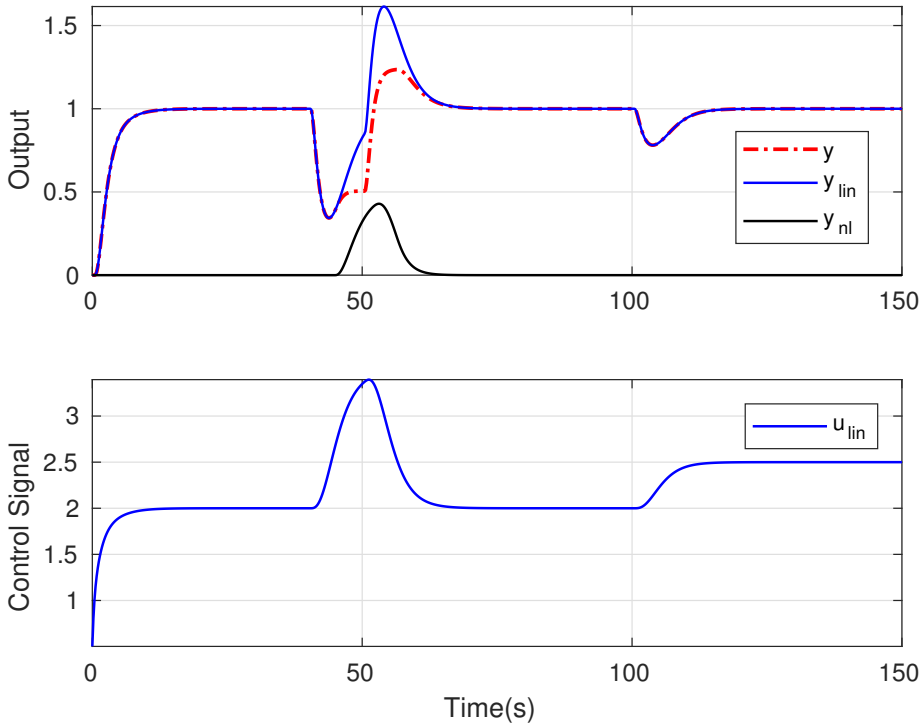

Source: The author.

4.1.1) to demonstrate the relationship between the $\mathscr{L}_2$ gain and the desired closed-loop poles. In order to generate a surface plot, one of the closed loop poles was fixed at $p_3 = 0.5$ while poles p_1 and p_2 were varied within the range $\begin{bmatrix} 0.04 & 0.96 \end{bmatrix}$. Then, it is clear that faster poles results in smaller $\mathscr{L}_2$ gains. This is due to the fact that the poles of the disturbance filter M_1 are equal to the poles of the set-point tracking H_{yr}.

Figure 21 – $\mathscr{L}_2$ gain dependence on set-point tracking poles - Example 3.

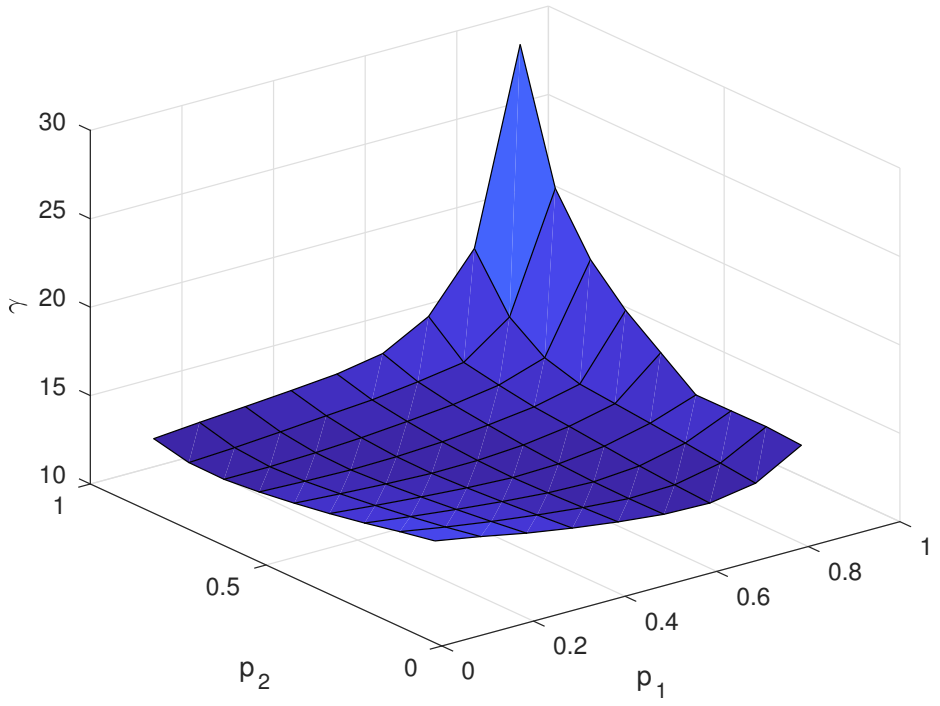

Source: The author.

5.1.4 Remarks on Stability

Although it is possible to guarantee global stability of the closed-loop system in the nominal case for first-order integrator processes (as stated by Theorem 2.3.1), none of the controllers used in Example 1 could make such guarantee by using Theorem 4.1.1 (which establishes stability for the nominal case) as no feasible solution was found. Therefore, the $\mathscr{L}_2$ gain was only presented for the stable second-order system in Example 3.

Nevertheless, feasible solutions were found using Corollaries 4.2.1, 4.2.3, 4.2.4 and 4.2.6 for the FOPDT system, as was presented in Example 2. A possible explanation for this is that the Corollaries which state the internal stability of the AWSDTC and SDTC were derived using the implementable structure of both controllers, where the subsystem S (3.15) is employed,

thus eliminating the integrator mode of G_n from the controller. This was verified by running LMIs from Theorem 4.1.1 using a very small negative pole for the fast-model G_n instead of the integrator mode of the real process model G, for which a feasible solution with small $\mathscr{L}_2$ gain was found. Corollaries 4.2.2 and 4.38, which establish stability conditions in the case of polytopic uncertainties, were not used in this Section as it was understood that the examples provided are enough to show the relation between tuning parameters and closed-loop robustness and performance of the AWSDTC. However, these Corollaries are available for use in future publication and are also a contribution of this work.

5.2 Experimental Data

To show the practical usefulness of the proposed anti-windup SDTC, the temperature control of a neonatal intensive care unit, depicted in Fig. 22, is presented. The plant model was obtained using a step-test identification procedure (NORMEY-RICO; CAMACHO, 2007) and is given by

$$Pn(s) = \frac{0.169e^{-7.8s}}{60s+1},$$

where the time is measured in minutes and the control signal is constrained within the range from 0 to 100 %. Using a sampling time of $T_s = 0.2(min)$, the discrete-time model is obtained as

$$Pn(z) = \frac{0.0005624}{z-0.9967}z^{-39}.$$

Figure 22 – Picture of the neonatal intensive care unit.

Source: The author.

The control parameters were set as $R(z) = 0$, $F(z) = f_0 = 74.89$ and $K_r = 80.8089$. It is important to notice that with this controller the nominal desired closed loop transfer function is

$$H_{yr}(z) = \frac{0.04545}{z - 0.9546} z^{-39}, \tag{5.2}$$

which was chosen to obtain a much faster set-point tracking response than the open-loop plant. Conventional PID controllers are not able to obtain such improvement as the one obtained with the SDTC.

The filter $V(z)$, with $b_0 = 26.82$, $b_1 = -26.49$ and $\beta = 0.9355$ was used to increase the system robustness with a properly measurement noise attenuation.

Experimental results using the proposed controller are shown in Fig. 23. The temperature set-point is 30^oC. Observe that, as expected, the settling time is close to 30 min with small oscillation, showing an undershoot of 0.5^oC due to unmodeled dynamics. It is important to note that even though the plant input became saturated during the first 20 minutes, the controller did not present windup issues.

Figure 23 – Experimental results: Temperature control of a NICU.

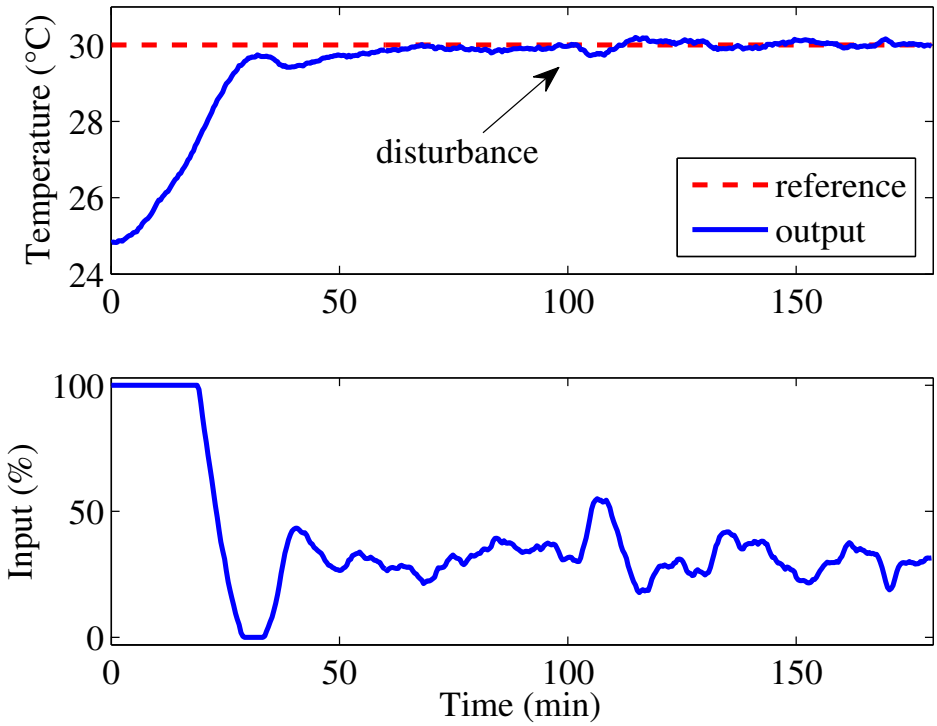

Source: The author.

According to the nominal desired closed loop transfer function, the expected settling

time for the unconstrained case is 20.7 min (5% criteria). However, due to the input saturation, the observed response in Fig. 23 has a settling time of approximately 30 min.

In order to assess the controller robustness, the front port holes of the NICU were opened between $t = 100$ min and $t = 105$ min. In this case, an undershoot of $0.3^{o}C$ occurred and the set-point was achieved once again within 12 min.

6 CONCLUSION

An anti-windup SDTC strategy applied to the control of stable and integrative plants has been presented. The proposed controller includes the saturation model in its structure and maintains the tuning simplicity of a conventional SDTC. However, in this case robustness filter must be chosen carefully in order to avoid windup problems. It was shown that disturbance rejection response of the proposed anti-windup SDTC during saturation events can present better results if compared to another anti-windup DTC schemes previously proposed in the literature.

Simulation results demonstrated that the proposed anti-windup SDTC is able to remain stable and present good time-response even in the presence of time-varying delays and norm-bounded uncertainties. Theorems that state robust global stability of the AWSDTC (and also the conventional SDTC) in the presence of time-varying delays, polytopic and norm-bounded uncertainties were provided in the form of LMIs. The relationship between the tuning parameters and the stability and performance of the proposed strategy was also demonstrated.

Finally, the developed experiment effectively assures that the proposed controller does not present windup issues, while keeps the good performance of a conventional SDTC. Due to its inherent simplicity, the proposed scheme is supposed to present great potential if implemented in commercial applications.

6.1 Recommendations for Future Work

In this thesis, global stability conditions were presented for the anti-windup SDTC. Although this analysis is useful as a first study, its employment is very limiting since it cannot be used for unstable open-loop plants. Therefore, it is of interest to relax these conditions to the case of regional stability, since most of the time in real life applications initial conditions are limited to a specific area of the $\mathbb{R}^n$, thus not being necessary to consider the whole space as the domain of attraction.

Another important point to comment is that in this thesis LMIs were used uniquely to provide proof of stability. Hence, a useful extension of the results provided herein would be to develop LMIs that can also be used for the design of the compensator. More specifically, FIR filters R and F could be designed to minimize the $\mathscr{L}_2$ gain.

In addition, this work was limited to the case of SISO systems. It is of theoretical importance to extend the results for MIMO systems with actuator saturation.

BIBLIOGRAPHY

ALBERTOS, P.; GARCÍA, P. Robust control design for long time-delay systems. **J Process Control**, v. 19, n. 10, p. 1640–1648, 2009.

ASTROM, K. J.; HANG, C. C.; LIM, B. C. A new smith predictor for controlling a process with a integrator and long dead-time. **IEEE Trans Autom Control**, v. 39, n. 2, p. 343–345, 1994.

BOYD, S.; El Ghaoui, L.; FERON, E.; BALAKRISHNAN, V. **Linear Matrix Inequalities in System and Control Theory**. Philadelphia, PA: SIAM, 1994. v. 15. (Studies in Applied Mathematics, v. 15). ISBN 0-89871-334-X.

BRIAT, C. **Linear Parameter-Varying and Time-Delay Systems**. [S.l.]: Springer Berlin Heidelberg, 2015.

CAMACHO, E. F.; BORDONS, C. **Model Predictive Control**. [S.l.]: Springer Verlag, 2004.

CHILALI, M.; GAHINET, P. H infin; design with pole placement constraints: an lmi approach. **IEEE Transactions on Automatic Control**, v. 41, n. 3, p. 358–367, Mar 1996. ISSN 0018-9286.

FLESCH, R. C. C.; NORMEY-RICO, J. E.; FLESCH, C. A. A unified anti-windup strategy for siso discrete dead-time compensators. **Control Engineering Practice**, v. 69, p. 50–60, 2017.

FRIDMAN, E. New lyapunov–krasovskii functionals for stability of linear retarded and neutral type systems. **Systems & Control Letters**, v. 43, n. 4, p. 309 – 319, 2001. ISSN 0167-6911.

FRIDMAN, E. **Introduction to Time-Delay Systems**. [S.l.]: Springer International Publishing, 2014. 68, 83, 247-251 p.

FRIDMAN, E. Tutorial on lyapunov-based methods for time-delay systems. **European Journal of Control**, v. 20, n. 6, p. 271 – 283, 2014. ISSN 0947-3580.

GARCÍA, P.; ALBERTOS, P. A new dead-time compensator to control stable and integrating processes with long dead-time. **Automatica**, v. 44, n. 4, p. 1062–1071, 2008.

GARCÍA, P.; ALBERTOS, P.; HAGGLUND, T. Control of unstable non-minimum-phase delayed systems. **J Process Control**, v. 16, n. 10, p. 1099–1111, 2006.

HESPANHA, J. P.; NAGHSHTABRIZI, P.; XU, Y. A survey of recent results in networked control systems. **Proceedings of the IEEE**, v. 95, n. 1, p. 138–162, Jan 2007. ISSN 0018-9219.

HIEN, L. V.; TRINH, H. New finite-sum inequalities with applications to stability of discrete time-delay systems. **Automatica**, v. 71, n. Supplement C, p. 197 – 201, 2016. ISSN 0005-1098.

HUBA, M. Comparing 2dof pi and predictive disturbance observer based filtered pi control. **J Process Control**, v. 23, p. 1379–1400, 2013.

HUBA, M. Robustness versus performance in pdo fpi control of the ipdt plant. In: **IEEE International Conference on Mechatronics**. Nagoya - Japan: [s.n.], 2015. p. 1379–1400.

HUBA, M.; TAPAK, P. Experimenting with the modified filtered smith predictors for fopdt plants. In: **Preprints of the 18th IFAC World Congress**. Milano - Italy: [s.n.], 2011. p. 2452–2457.

KAYA, I. A new smith predictor and controller for control of processes with long dead time. **ISA Trans**, v. 42, p. 101–110, 2003.

KHALIL, H. **Nonlinear Systems**. [S.l.]: Prentice Hall, 2002. (Pearson Education). ISBN 9780130673893.

KIRTANIA, K.; CHOUDHURY, M. A. A. S. Set point weighted modified smith predictor for integrating and double integrating processes with time delay. **J Process Control**, v. 22, n. 3, p. 612–625, 2012.

KOTHARE, M. V.; CAMPO, P. J.; MORARI, M.; NETT, C. N. A unified frame-work for the study of anti-windup designs. **Automatica**, v. 30, n. 12, p. 1869–1883, 1994.

LAMNABHI-LAGARRIGUE, F.; ANNASWAMY, A.; ENGELL, S.; ISAKSSON, A.; KHARGONEKAR, P.; MURRAY, R. M.; NIJMEIJER, H.; SAMAD, T.; TILBURY, D.; HOF, P. V. den. Systems & control for the future of humanity, research agenda: Current and future roles, impact and grand challenges. **Annual Reviews in Control**, v. 43, n. Supplement C, p. 1 – 64, 2017. ISSN 1367-5788.

LASSERRE, J. B. Reachable, controllable sets and stabilizing control of constrained linear systems. **Automatica**, v. 29, n. 2, p. 531–536, 1993.

LIU, J.; ZHANG, J. Note on stability of discrete-time time-varying delay systems. **IET Control Theory Applications**, v. 6, n. 2, p. 335–339, January 2012. ISSN 1751-8644.

LOFBERG, J. Yalmip : a toolbox for modeling and optimization in matlab. In: **2004 IEEE International Conference on Robotics and Automation (IEEE Cat. No.04CH37508)**. [S.l.: s.n.], 2004. p. 284–289.

LOUISELL, J. Delay diferential systems with time-varying delay: New directions for stability theory. **Kybernetika**, v. 37, n. 3, p. 239 – 252, 2001.

MATAUŠEK, M. R.; MICIĆ", A. D. A modified smith predictor for controlling a process with a integrator and long dead-time. **IEEE Trans Autom Control**, v. 41, n. 8, p. 1199–1203, 1996.

MATAUŠEK, M. R.; MICIĆ, A. D. On the modified smith predictor for controlling a process with a integrator and long dead-time. **IEEE Trans on Autom Control**, v. 44, n. 8, p. 1603–1606, 1999.

MATAUŠEK, M. R.; RIBIĆ, A. I. Control of stable, integrating and unstable processes by the modified smith predictor. **J Process Control**, v. 22, n. 1, p. 338–343, 2012.

NORMEY-RICO, J. E.; CAMACHO, E. F. **Control of Dead-time Processes**. Berlin: Springer, 2007.

NORMEY-RICO, J. E.; CAMACHO, E. F. Simple robust dead-time compensator for first-order plus dead-time unstable processes. **Ind Eng Chem Res**, v. 47, n. 14, p. 4784–4790, 2008.

PAPACHRISTODOULOU, A.; PEET, M. M.; NICULESCU, S. I. Stability analysis of linear systems with time-varying delays: Delay uncertainty and quenching. In: **2007 46th IEEE Conference on Decision and Control**. [S.l.: s.n.], 2007. p. 2117–2122. ISSN 0191-2216.

PARK, P.; KO, J. W.; JEONG, C. Reciprocally convex approach to stability of systems with time-varying delays. **Automatica**, v. 47, n. 1, p. 235 – 238, 2011. ISSN 0005-1098.

RAO, A. S.; CHIDAMBARAM, M. Analytical design of modified smith predictor in a two-degrees-of-freedom control scheme for second order unstable processes with time delay. **ISA Trans**, v. 47, n. 4, p. 407–419, 2008.

RAO, A. S.; RAO, V. S. R.; CHIDAMBARAM, M. Set point weighted modified smith predictor for integrating and double integrating processes with time delay. **ISA Trans**, v. 46, n. 1, p. 59–71, 2007.

SANTOS, T. L. M.; BOUTURA, P. E. A.; NORMEY-RICO, J. E. Dealing with noise in unstable dead-time process control. **J Process Control**, v. 20, n. 7, p. 840–847, 2010.

SEURET, A.; GOUAISBAUT, F.; FRIDMAN, E. Stability of discrete-time systems with time-varying delays via a novel summation inequality. **IEEE Transactions on Automatic Control**, v. 60, n. 10, p. 2740–2745, Oct 2015. ISSN 0018-9286.

SHAO, H.; HAN, Q. L. New stability criteria for linear discrete-time systems with interval-like time-varying delays. **IEEE Transactions on Automatic Control**, v. 56, n. 3, p. 619–625, March 2011. ISSN 0018-9286.

SKOGESTAD, S.; POSTLETHWAITE, I. **Multivariable Feedback Control: Analysis and Design**. [S.l.]: Wiley, 2005. ISBN 047001167X.

SMITH, O. J. M. Closed control of loops with dead-time. **Chem Eng Progress**, v. 53, p. 217–219, 1957.

SONTAG, E. D. An algebraic approach to bounded controllability of linear systems. **Int. J. Control**, v. 39, n. 1, p. 181–188, 1984.

SUN, J.; CHEN, J. A survey on lyapunov-based methods for stability of linear time-delay systems. **Frontiers of Computer Science**, v. 11, n. 4, p. 555–567, Aug 2017. ISSN 2095-2236.

TARBOURIECH G. GARCIA, J. M. G. d. S. J. I. Q. S. **Stability and Stabilization of Linear Systems with Saturating Actuators**. London: Springer, 2011. 19-20 p.

TARBOURIECH, S.; TURNER, M. Anti-windup design: an overview of some recent advances and open problems. **IET Control Theory Applications**, v. 3, n. 1, p. 1–19, January 2009. ISSN 1751-8644.

TORRICO, B. C.; CAVALCANTE, M. U.; BRAGA, A. P. S.; ALBUQUERQUE, A. A. M.; NORMEY-RICO, J. E. Simple tuning rules for dead-time compensation of stable, integrative, and unstable first-order dead-time processes. **Ind Eng Chem Res**, v. 52, p. 11646–11654, 2013.

TORRICO, B. C.; CORREIA, W. B.; NOGUEIRA, F. G. Simplified dead-time compensator for multiple delay siso systems. **ISA Transactions**, v. 60, p. 254–261, 2016.

TURNER, G. H. M. C.; POSTLETHWAITE, I. **Advanced Strategies in Control Systems with Input and Output Constraints**. Berlin: Springer, 2007. 127-128 p.

WESTON, P. F.; POSTLETHWAITE, I. Linear conditioning for systems containing saturating actuators. **Automatica**, v. 36, n. 9, p. 1347 – 1354, 2000. ISSN 0005-1098.

XIE, L. Output feedback h∞ control of systems with parameter uncertainty. **International Journal of Control**, Taylor & Francis, v. 63, n. 4, p. 741–750, 1996.

YANG, Y.; SONTAG, E. D.; SUSSMANN, H. J. Global stabilization of linear discrete-time systems with bounded feedback. **Systems & Control Letters**, v. 30, n. 5, p. 273 – 281, 1997. ISSN 0167-6911.

ZHANG, B.; XU, S.; ZOU, Y. Improved stability criterion and its applications in delayed controller design for discrete-time systems. **Automatica**, v. 44, n. 11, p. 2963 – 2967, 2008. ISSN 0005-1098.

ZHANG, M.; JIANG, C. Problem and its solution for actuator saturation of integrating process with dead time. **ISA Trans.**, v. 47, p. 80–84, 2008.

ZHOU, K.; DOYLE, J. C.; GLOVER, K. **Robust and Optimal Control**. Upper Saddle River, NJ, USA: Prentice-Hall, Inc., 1996. ISBN 0-13-456567-3.

ZHU, X.-L.; YANG, G.-H. Jensen inequality approach to stability analysis of discrete-time systems with time-varying delay. In: **2008 American Control Conference**. [S.l.: s.n.], 2008. p. 1644–1649. ISSN 0743-1619.

APPENDIX A – DEMONSTRATION OF LINEAR AND NONLINEAR LOOPS DECOUPLING

Obtaining Figure 12 (Section 4.1)

In order to find an equivalent representation of Figure 11 which decouples the linear and nonlinear loops, signals j, y, x and u are defined as

$$j = Ssat(u), \tag{A.1}$$

$$y = P[sat(u) + q] + n, \tag{A.2}$$

$$x = j + Vy, \tag{A.3}$$

$$u = K_r r_{ef} - x = K_r r_{ef} - j - Vy. \tag{A.4}$$

Then,

$$y = P[sat(K_r r_{ef} - j - Vy) + q] + n, \text{ and} \tag{A.5}$$

$$j = Ssat(K_r r_{ef} - j - Vy). \tag{A.6}$$

Since it is desired to separate the linear and the nonlinear loops, the following identities must hold true

$$y = y_{lin} - y_{nl}, \text{ and} \tag{A.7}$$

$$j = j_{lin} - j_{nl}, \tag{A.8}$$

where subscripts *lin* and *nl* denote the linear and nonlinear components of y and j, respectively. Using the identity in Equation 2.85, one can rewrite Equations (A.7) and (A.8) as

$$y = P[(K_r r_{ef} - j - Vy) - Dz(K_r r_{ef} - j - Vy) + q] + n, \text{ and} \tag{A.9}$$

$$j = S[(K_r r_{ef} - j - Vy) - Dz(K_r r_{ef} - j - Vy)]. \tag{A.10}$$

By substituting Equations (A.7) and (A.8) into the right side of Equations (A.9) and (A.10), it is obtained

$$y = P[(K_r ref - j_{lin} - Vy_{lin}) + q] + n - P[dz(K_r r_{ef} - j_{lin} - Vy_{lin} + j_{nl} + Vy_{nl}) - (Vy_{nl} + j_{nl})] \tag{A.11}$$

and

$$j = S[(K_r r_{ef} - j_{lin} - Vy_{lin})] - S[dz(K_r r_{ef} - j_{lin} - Vy_{lin} + j_{nl} + Vy_{nl}) - (Vy_{nl} + j_{nl})]. \tag{A.12}$$

By defining

$$u_{lin} = K_r r_{ef} - j_{lin} - Vy_{lin}, \tag{A.13}$$

$$y_{lin} = P[u_{lin} + q] + n, \tag{A.14}$$

$$ud = -(j_{nl} + Vy_{nl}), \tag{A.15}$$

$$\tilde{u} = Dz(u_{lin} - ud), \tag{A.16}$$

$$y_{nl} = P(\tilde{u} + u_d), \tag{A.17}$$

$j_{lin} = Su_{lin}$, and (A.18)

$j_{nl} = S(\tilde{u} + u_d)$, (A.19)

the decoupled structure in Figure 24 is obtained.

Figure 24 – Decoupling between linear and nonlinear loops - simplified generic case.

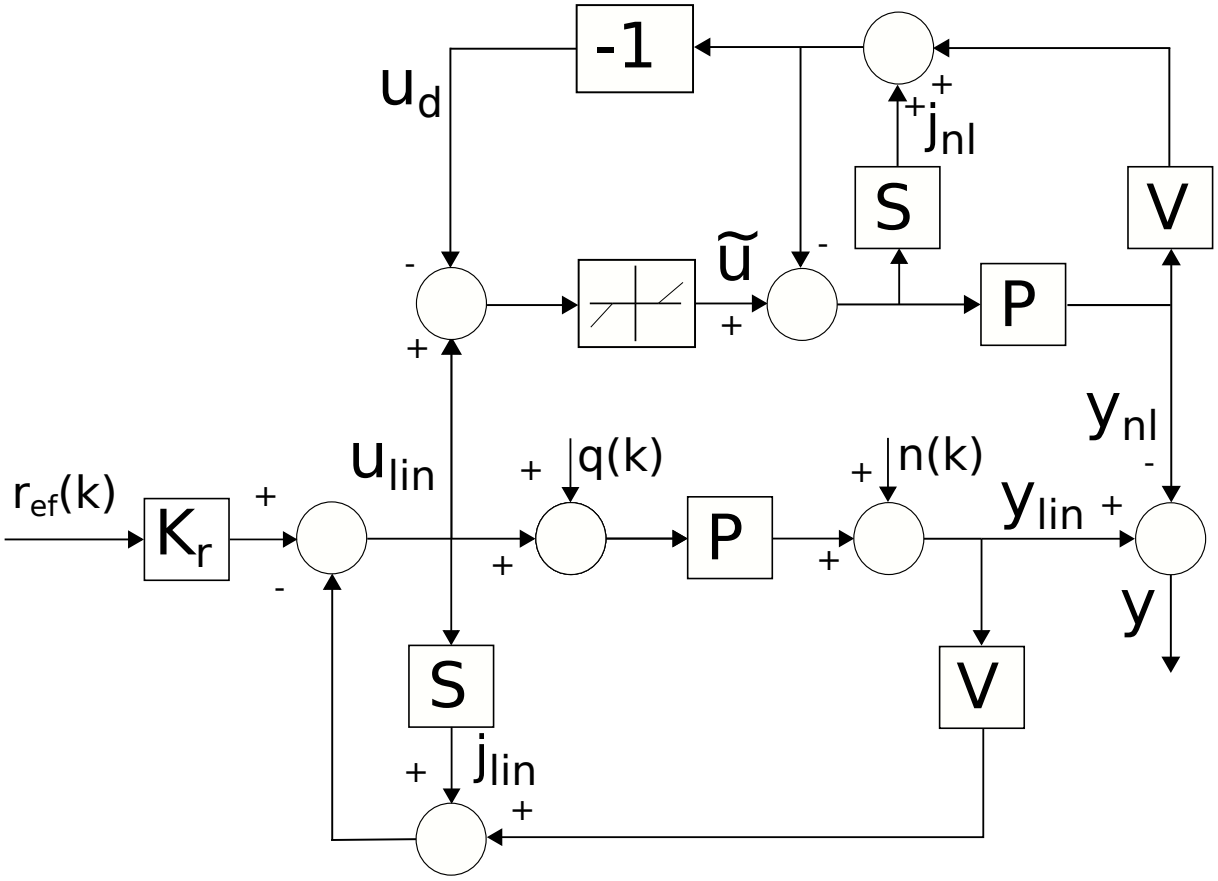

Source: The author.

Using the definition of $S(z)$ (Equation (3.15)) the nonlinear loop, defined by the mapping from y_{lin} to y_{nl}, can be redrawn as in Figure 25.

Notice that when $P(z) = P_n(z)$ (for the nominal analysis) signal $e(k) = 0$ and the structure in Figure 25 can be further simplified to the structure in Figure 26.

From Figure 26 note that, in the nominal case, the nonlinear loop depends only upon FIR filters $R(z)$ and $F(z)$ and the process model $P_n(z)$. Robustness filter $V(z)$ only impacts the nonlinear loop in the case of uncertainties in the process model.

Figure 25 – Decoupling between linear and nonlinear loops - non simplified generic case.

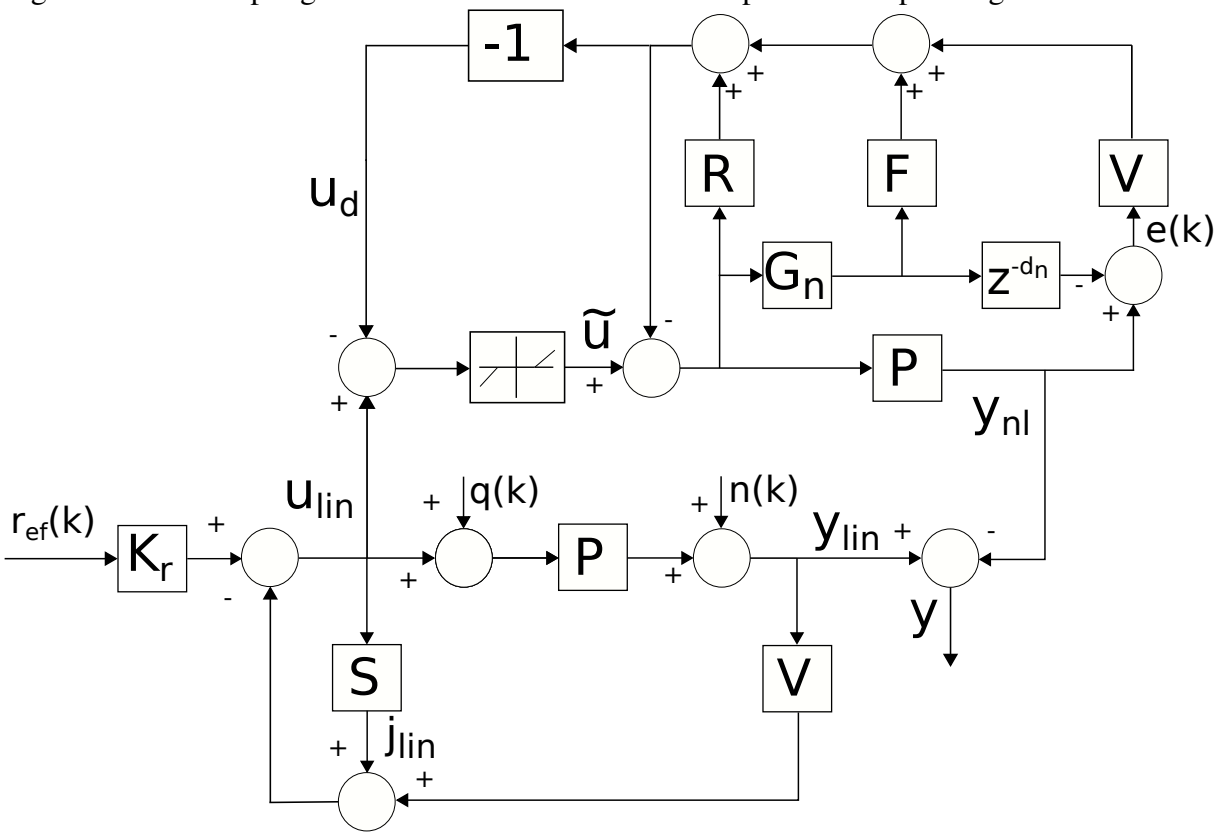

Source: The author.

Finally, in order to obtain the structure presented in Figure 12 (Section 4.1) note that

$$M_1(z) = \frac{y_d}{\tilde{u}} = \frac{G_n(z)}{1+R(z)+G_n(z)F(z)}, \text{ and} \tag{A.20}$$

$$M_2(z) = \frac{u_d}{\tilde{u}} = -\frac{R(z)+G_n(z)F(z)}{1+R(z)+G_n(z)F(z)}. \tag{A.21}$$

Demonstration of mapping $\tau_{pn} : u_{lin} \rightarrow y_d$ (Section 4.1)

From Figure 26 the following state space equations to describe the mapping $\tau_{pn} : u_{lin} \rightarrow y_d$ are initially written

$$\begin{cases} x_n(k+1) = A_p x_n(k) + B_p(\tilde{u} + u_d) \\ y_d(k) = C_p x_n(k) \end{cases} \tag{A.22}$$

Figure 26 – Decoupling between linear and nonlinear loops - nominal case.

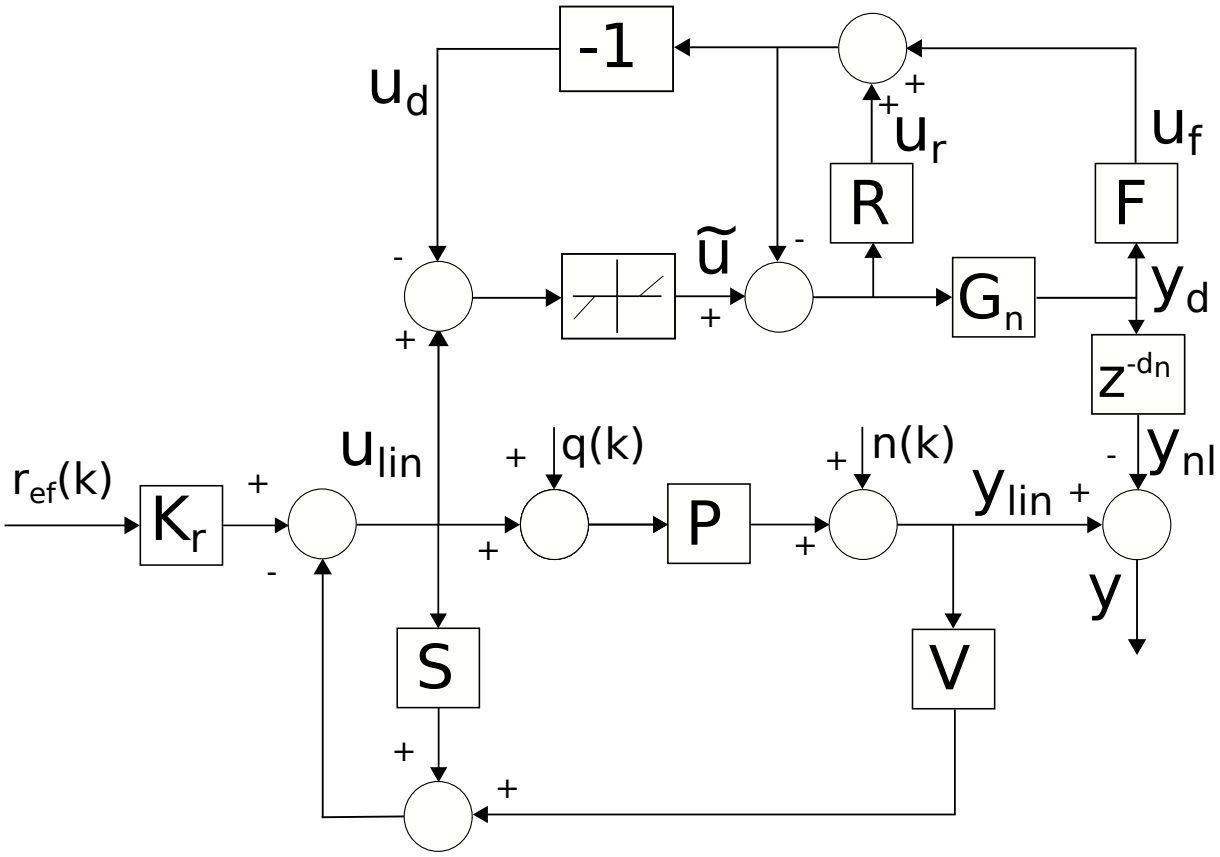

Source: The author.

$$\begin{cases} x_f(k+1) = A_F x_f(k) + B_F y_d \\ u_f(k) = C_F x_f(k) + D_F y_d \end{cases} \tag{A.23}$$

$$\begin{cases} x_r(k+1) = A_R x_r(k) + B_R(\tilde{u} + u_d) \\ u_f(k) = C_R x_r(k) + D_R(\tilde{u} + u_d) \end{cases} \tag{A.24}$$

Note that $u_d = -u_f - u_r$. Then, using the definitions for u_f, u_r and y_d

$$u_d = -\Delta C_F x_f - \Delta D_F C_p x_n(k) - \Delta C_R x_r - \Delta D_R \tilde{u}, \tag{A.25}$$

where $\Delta = \left[I - D_R\right]$. Then, by substituting Equation (A.25) into $x_n(k+1)$ and $x_r(k+1)$, it is obtained

$$x_n(k+1) = (A_p - B_p \Delta D_F C_p) x_n(k) - B_p \Delta C_F x_f - B_p \Delta C_R x_r + (B_p - B_p \Delta D_R)\tilde{u}, \text{ and} \tag{A.26}$$

$$x_r(k+1) = (A_R - B_R\Delta C_R)x_r(k) - B_r\Delta D_F C_p x_n - B_R\Delta C_F x_f + (B_R - B_R\Delta D_R)\tilde{u}. \tag{A.27}$$

In addition, substitution of y_d into $x_f(k+1)$ leads to

$$x_f(k+1) = A_F x_f + B_F C_p x_n. \tag{A.28}$$

Finally, by defining $x(k) = \begin{bmatrix} x_n(k)^T & x_f(k)^T & x_r(k)^T \end{bmatrix}^T$ the the mapping $\tau_{pn} : u_{lin} \rightarrow y_d$ is obtained as

$$\tau_{pn} \triangleq \begin{cases} x(k+1) = \bar{A}x(k) + \bar{B}\tilde{u} \\ u_d = \bar{C_2}x(k) + \bar{D}_2\tilde{u} \\ y_d = \bar{C_1}x(k) \\ \tilde{u} = Dz(u_{lin} - u_d) \end{cases} \tag{A.29}$$

where

$$\bar{A} = \begin{bmatrix} A_p - B_p\Delta D_F C_p & -B_p\Delta C_F & -B_p\Delta C_R \\ B_F C_p & A_F & 0 \\ -B_R\Delta D_F C_p & -B_R\Delta C_F & A_R - B_R\Delta C_R \end{bmatrix},$$

$$\bar{B} = \begin{bmatrix} B_p - B_p\Delta D_R \\ 0 \\ B_R - B_R\Delta D_R \end{bmatrix},$$

$$\bar{C_1} = \begin{bmatrix} C_p & 0 & 0 \end{bmatrix}, \quad \bar{C_2} = \begin{bmatrix} -\Delta D_F C_p & -\Delta C_F & -\Delta C_R \end{bmatrix},$$

$$\bar{D_2} = \begin{bmatrix} -\Delta D_R \end{bmatrix}, \quad \Delta = \begin{bmatrix} I - D_R \end{bmatrix}.$$